Supplemental Material Figures S4 to S8, Smith and Edwards 2020, Improved status and trend estimates from the North American Breeding Bird Survey using a Bayesian hierarchical generalized additive model

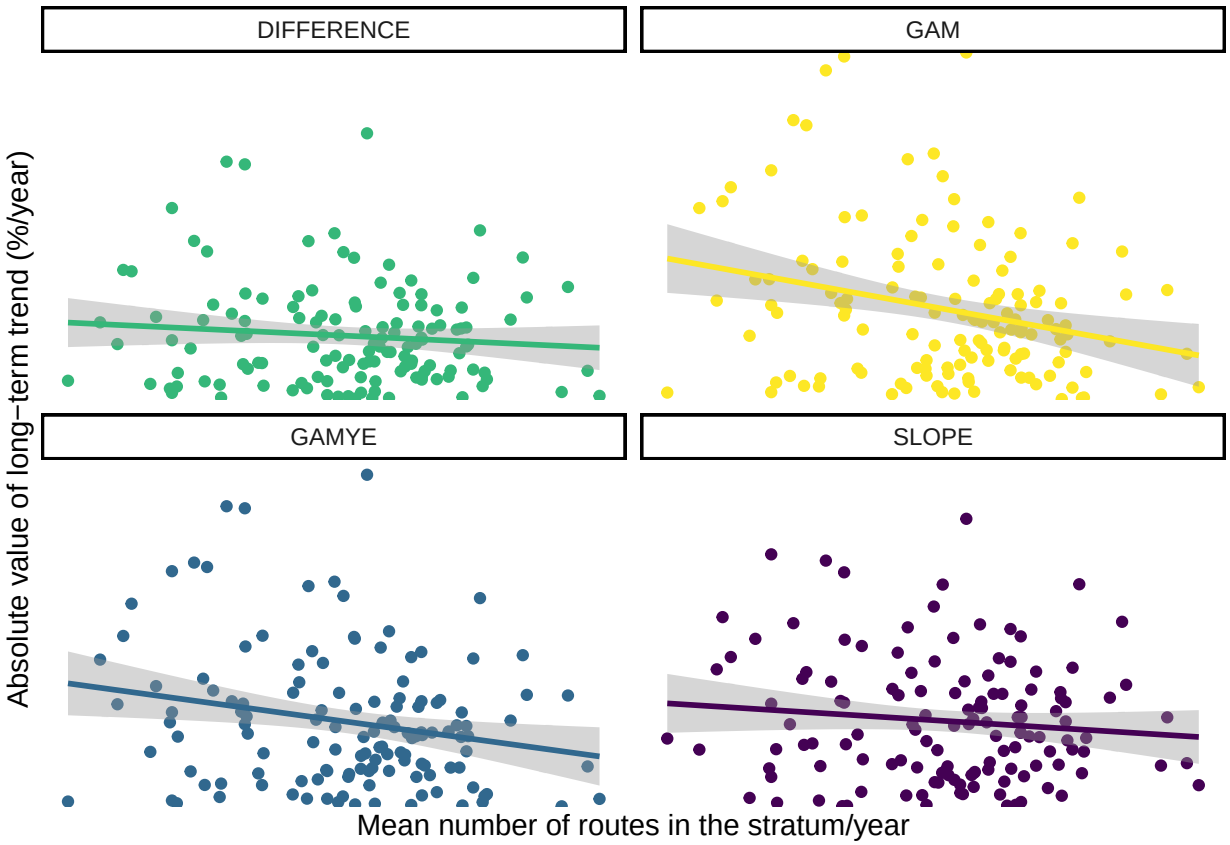

Figure 1: S4.A: Relationship between the absolute value of estimated long-term trends (1966-2018) and the amount of data in each stratum, from the four models compared here for American Kestrel.

```
## Warning: Removed 11 rows containing missing values (geom_smooth).
```

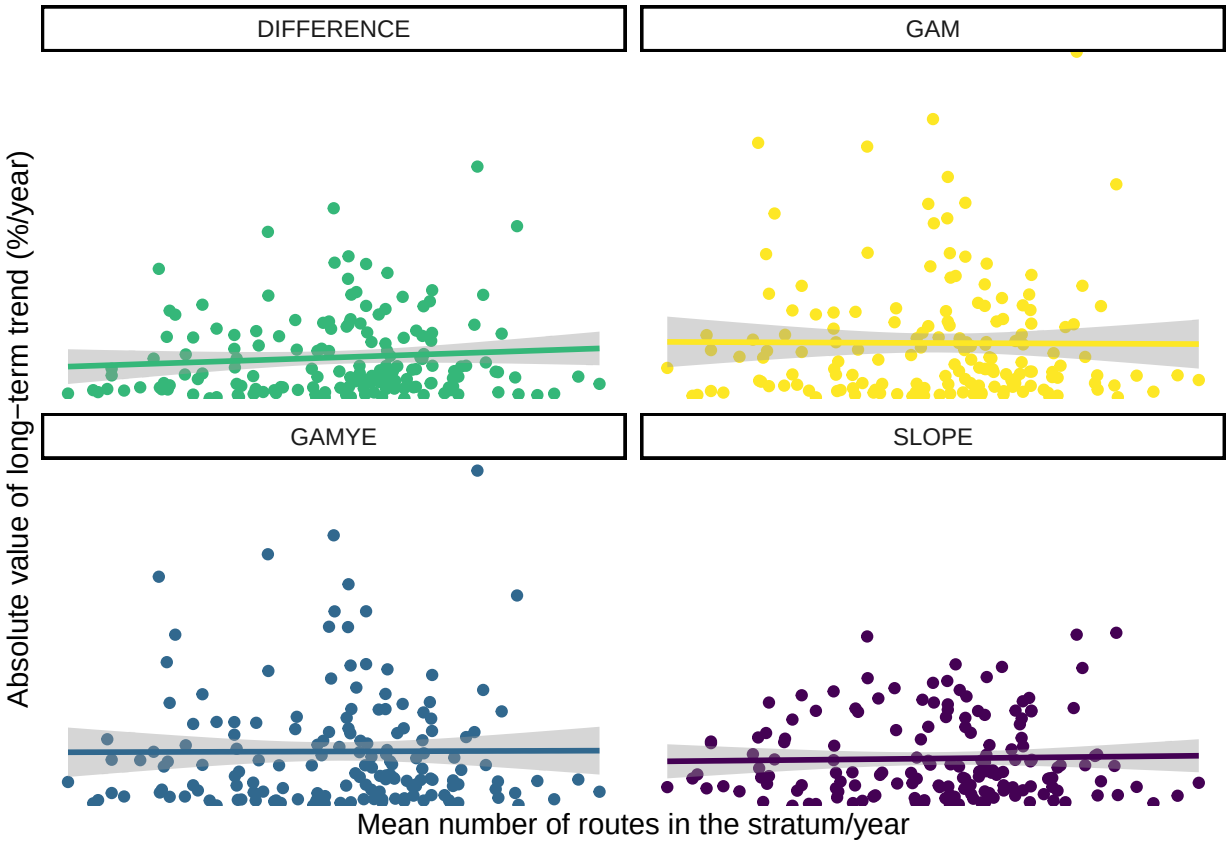

Figure 2: S4.B: Relationship between the absolute value of estimated long-term trends (1966-2018) and the amount of data in each stratum, from the four models compared here for Barn Swallow.

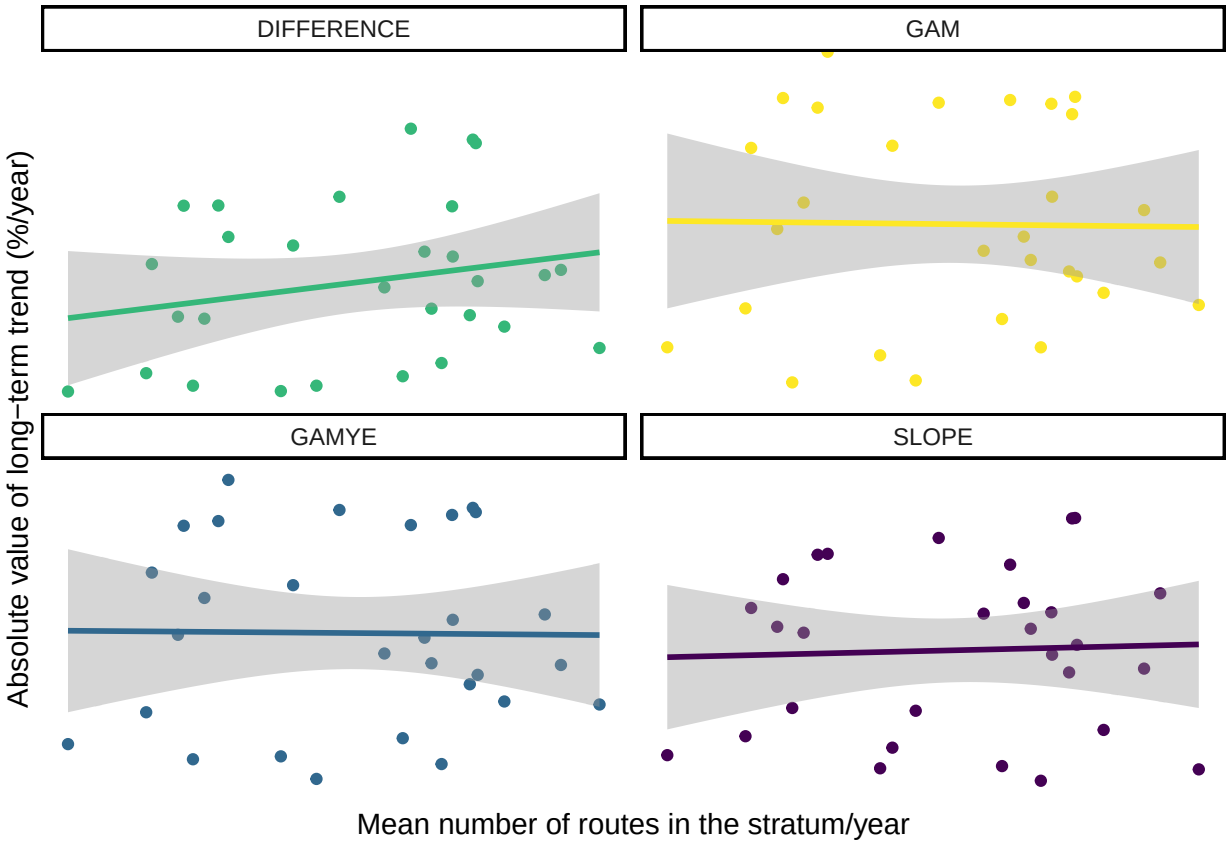

Figure 3: S4.C: Relationship between the absolute value of estimated long-term trends (1966-2018) and the amount of data in each stratum, from the four models compared here for Canada Warbler.

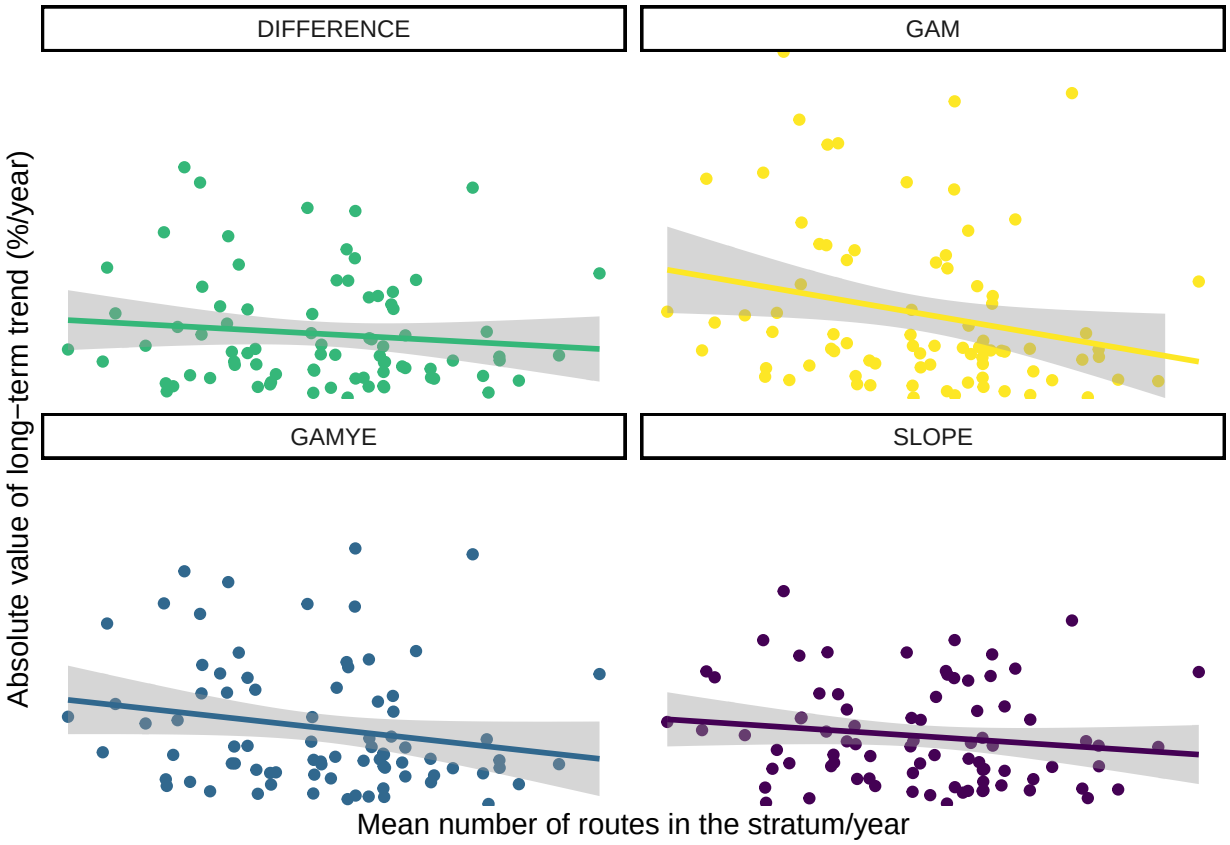

Figure 4: S4.D: Relationship between the absolute value of estimated long-term trends (1966-2018) and the amount of data in each stratum, from the four models compared here for Carolina Wren.

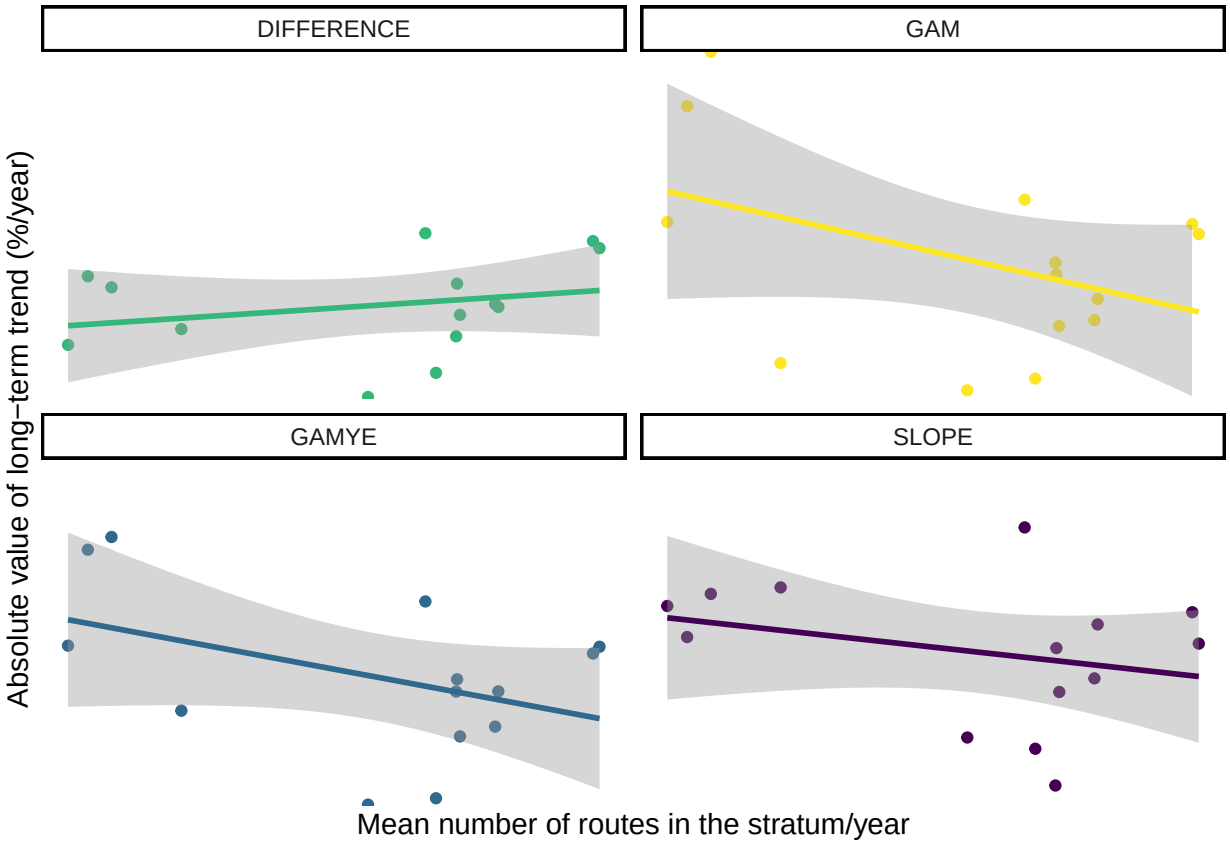

Figure 5: S4.E: Relationship between the absolute value of estimated long-term trends (1966-2018) and the amount of data in each stratum, from the four models compared here for Chestnut-collared Longspur.

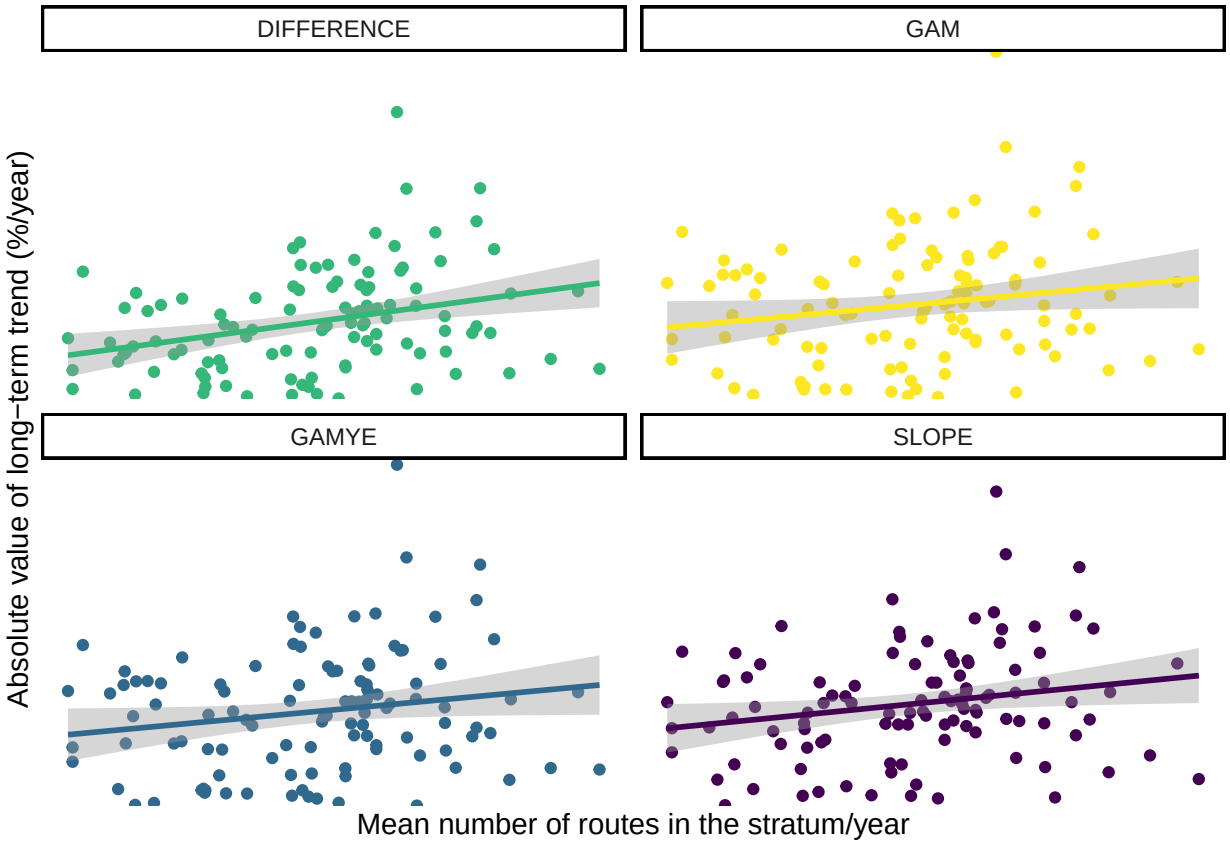

Figure 6: S4.F: Relationship between the absolute value of estimated long-term trends (1966-2018) and the amount of data in each stratum, from the four models compared here for Chimney Swift.

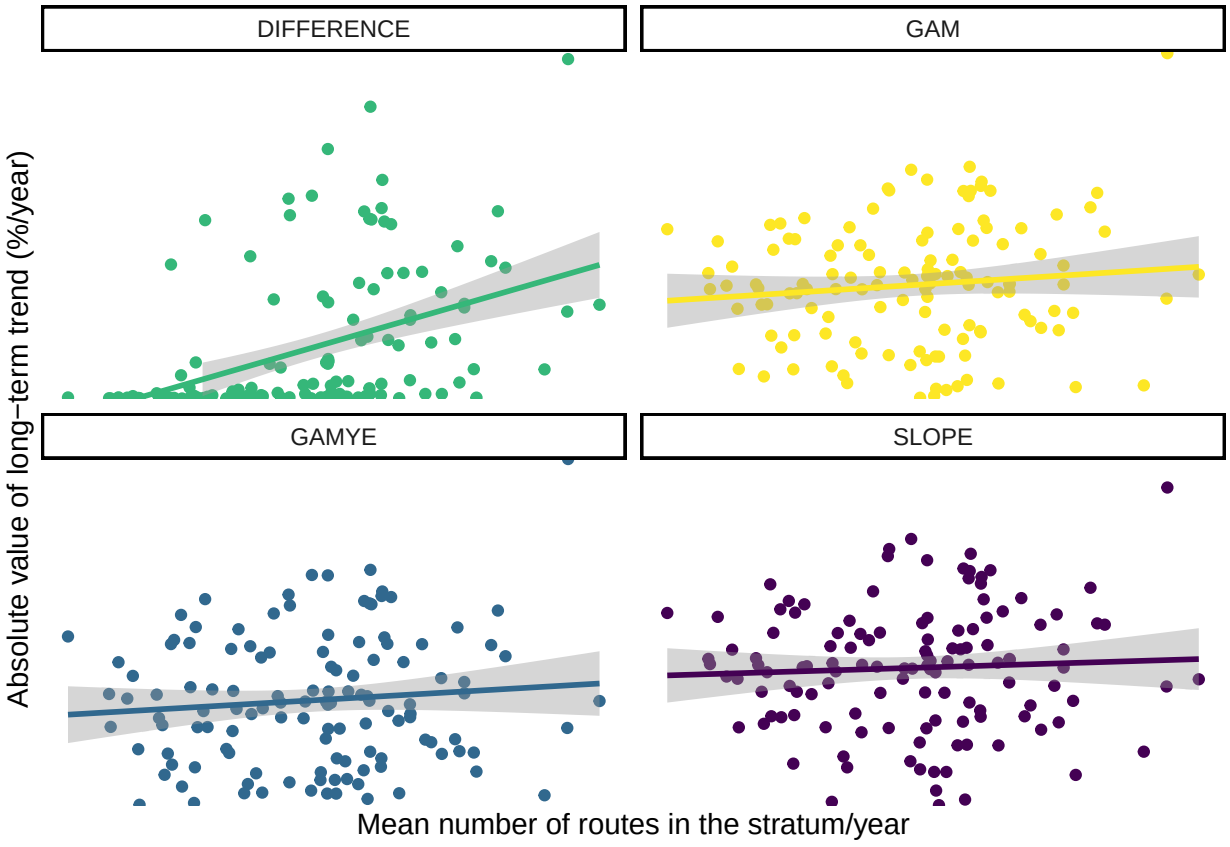

Figure 7: S4.G: Relationship between the absolute value of estimated long-term trends (1966-2018) and the amount of data in each stratum, from the four models compared here for Cooper's Hawk.

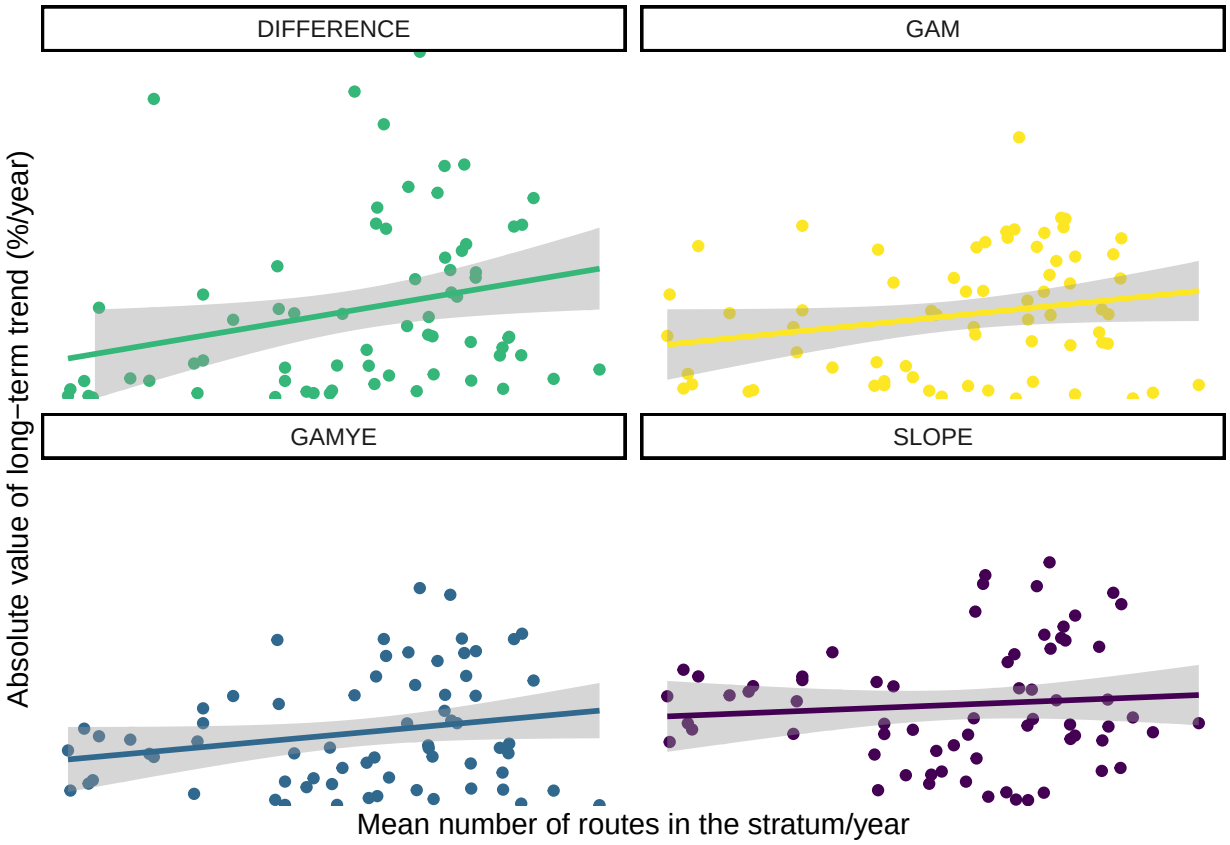

Figure 8: S4.H: Relationship between the absolute value of estimated long-term trends (1966-2018) and the amount of data in each stratum, from the four models compared here for Pine Siskin.

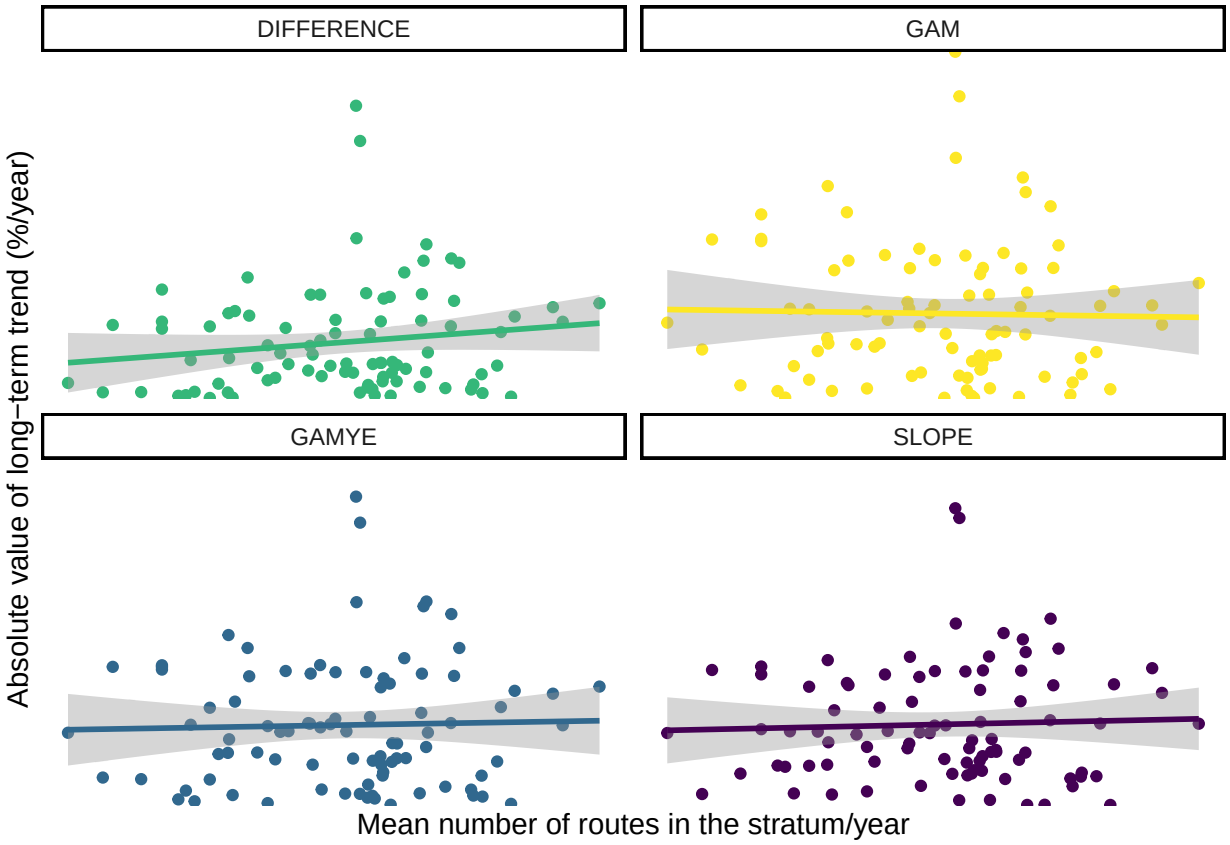

Figure 9: S4.I: Relationship between the absolute value of estimated long-term trends (1966-2018) and the amount of data in each stratum, from the four models compared here for Ruby-throated Hummingbird.

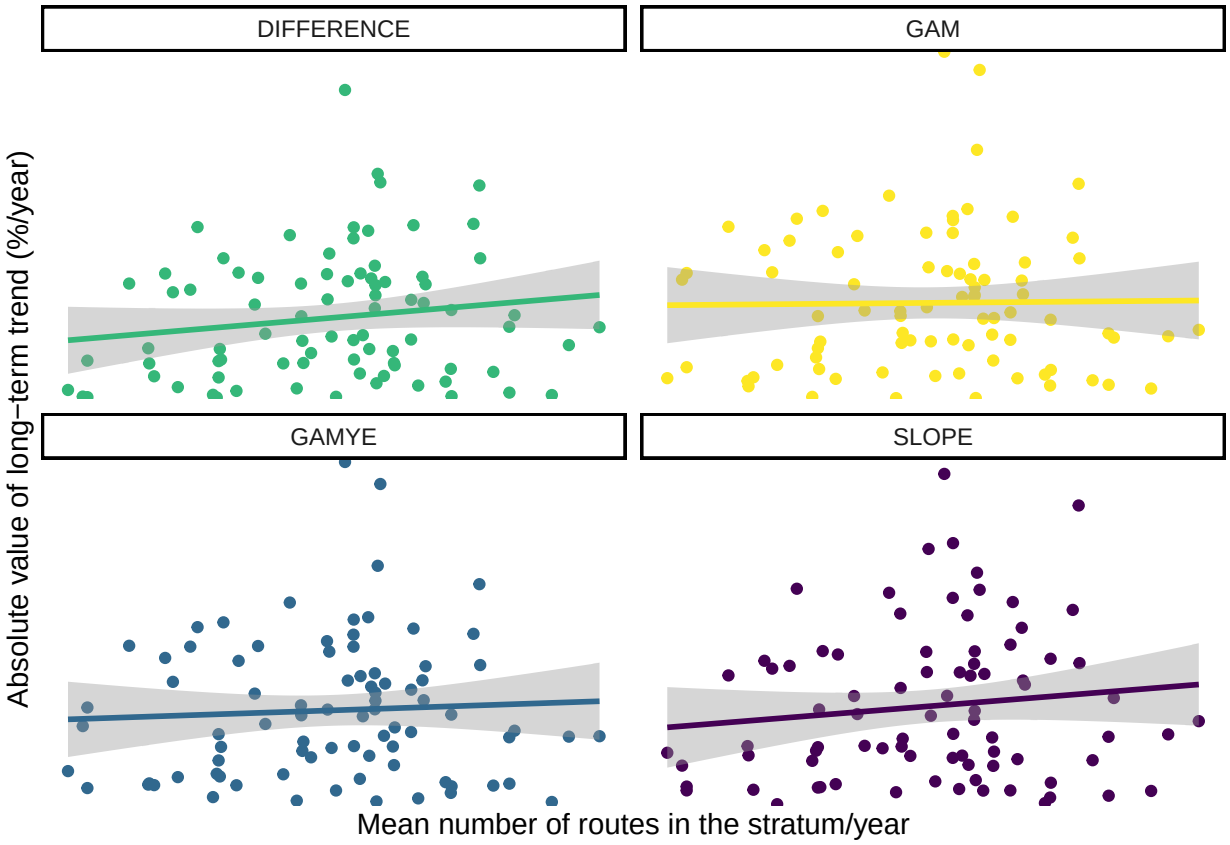

Figure 10: S4.J: Relationship between the absolute value of estimated long-term trends (1966-2018) and the amount of data in each stratum, from the four models compared here for Wood Thrush.

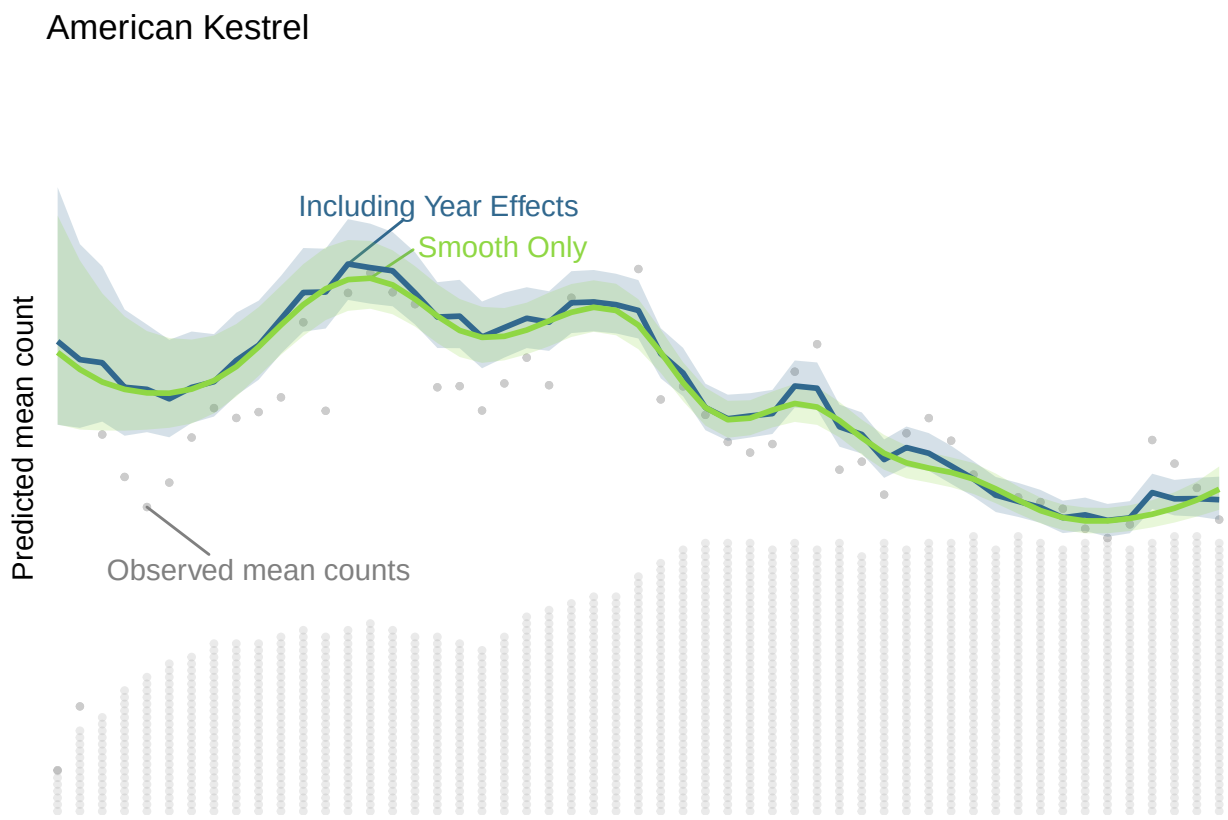

Figure 11: S5.A: Decomposition of the survey-wide population trajectory for American Kestrel from the GAMYE, showing the full trajectory (Including Year Effects) and the isolated smooth component (Smooth Only), which can be used to estimate population trends that are less sensitive to the particular year in which they are estimated. The stacked dots along the x axis indicate the approximate number of BBS counts used in the model; each dot represents 50 counts.

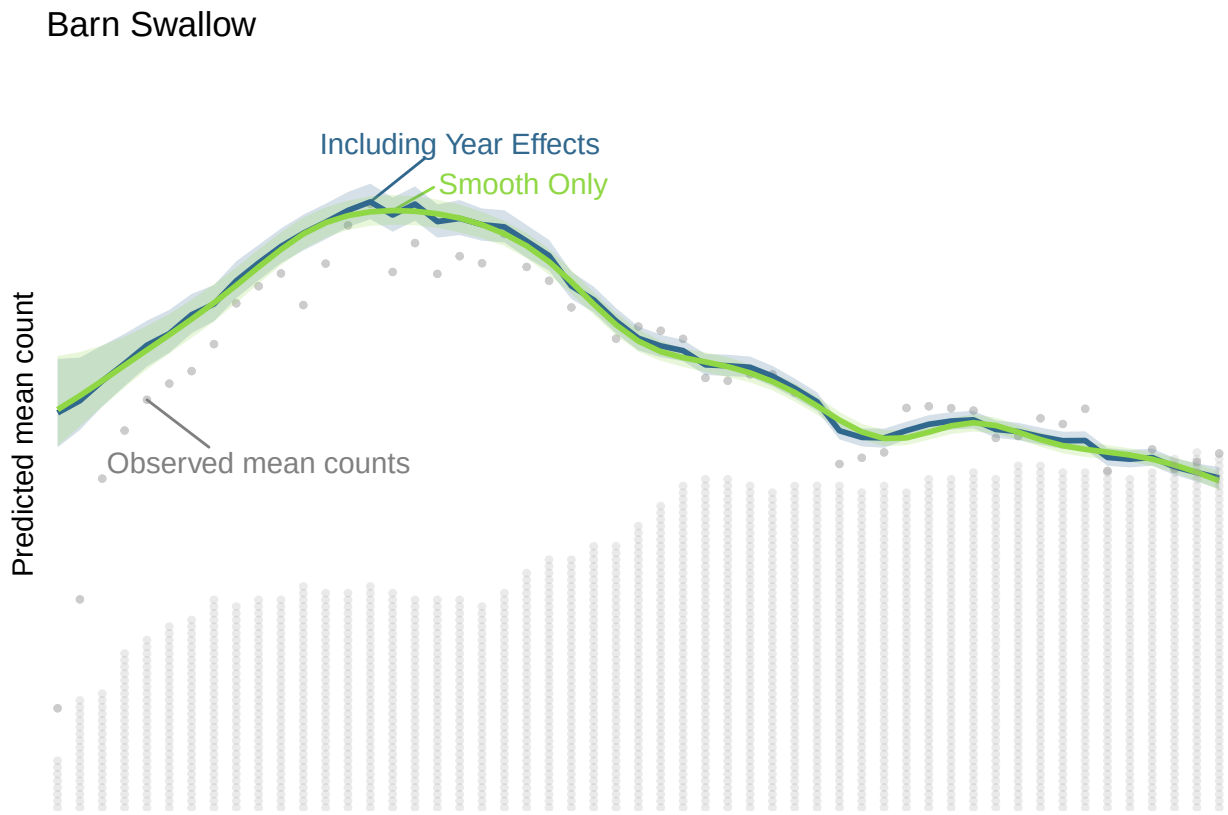

Figure 12: S5.B: Decomposition of the survey-wide population trajectory for Barn Swallow from the GAMYE, showing the full trajectory (Including Year Effects) and the isolated smooth component (Smooth Only), which can be used to estimate population trends that are less sensitive to the particular year in which they are estimated. The stacked dots along the x axis indicate the approximate number of BBS counts used in the model; each dot represents 50 counts.

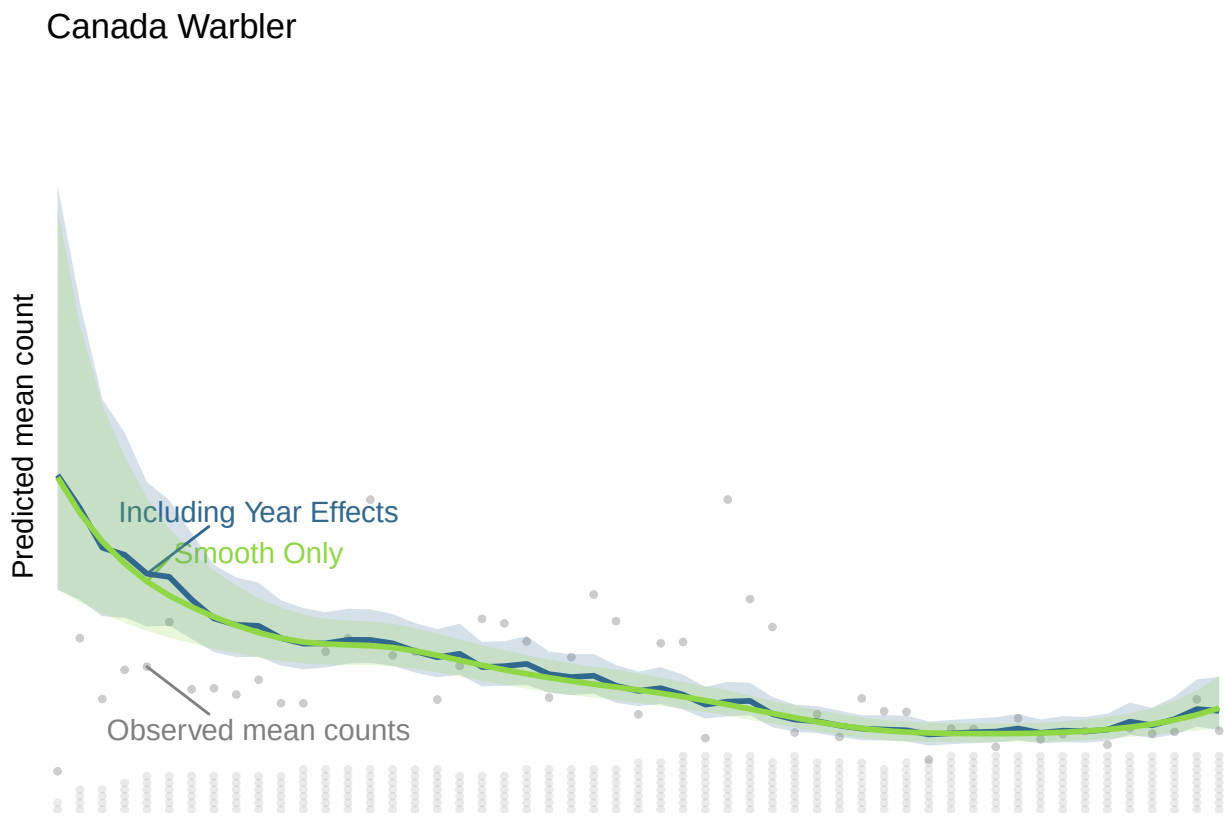

Figure 13: S5.C: Decomposition of the survey-wide population trajectory for Canada Warbler from the GAMYE, showing the full trajectory (Including Year Effects) and the isolated smooth component (Smooth Only), which can be used to estimate population trends that are less sensitive to the particular year in which they are estimated. The stacked dots along the x axis indicate the approximate number of BBS counts used in the model; each dot represents 50 counts.

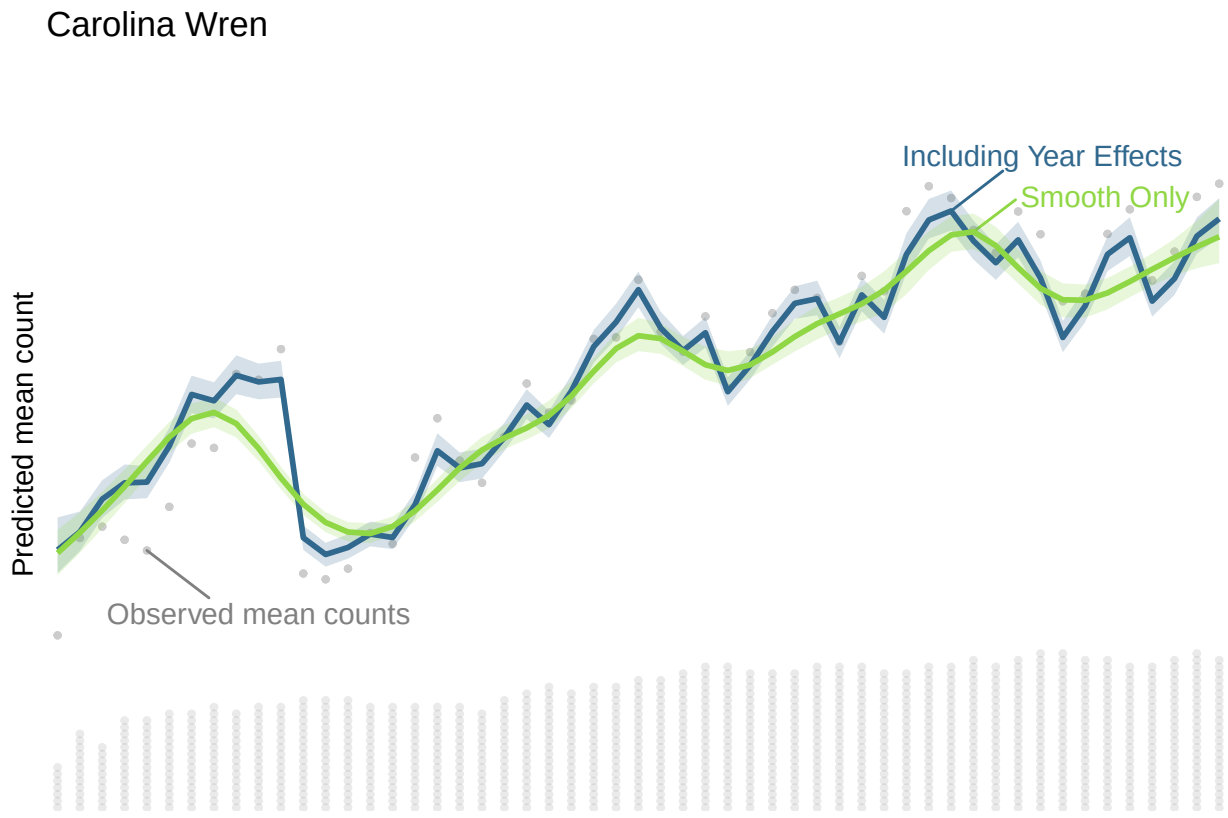

Figure 14: S5.D: Decomposition of the survey-wide population trajectory for Carolina Wren from the GAMYE, showing the full trajectory (Including Year Effects) and the isolated smooth component (Smooth Only), which can be used to estimate population trends that are less sensitive to the particular year in which they are estimated. The stacked dots along the x axis indicate the approximate number of BBS counts used in the model; each dot represents 50 counts.

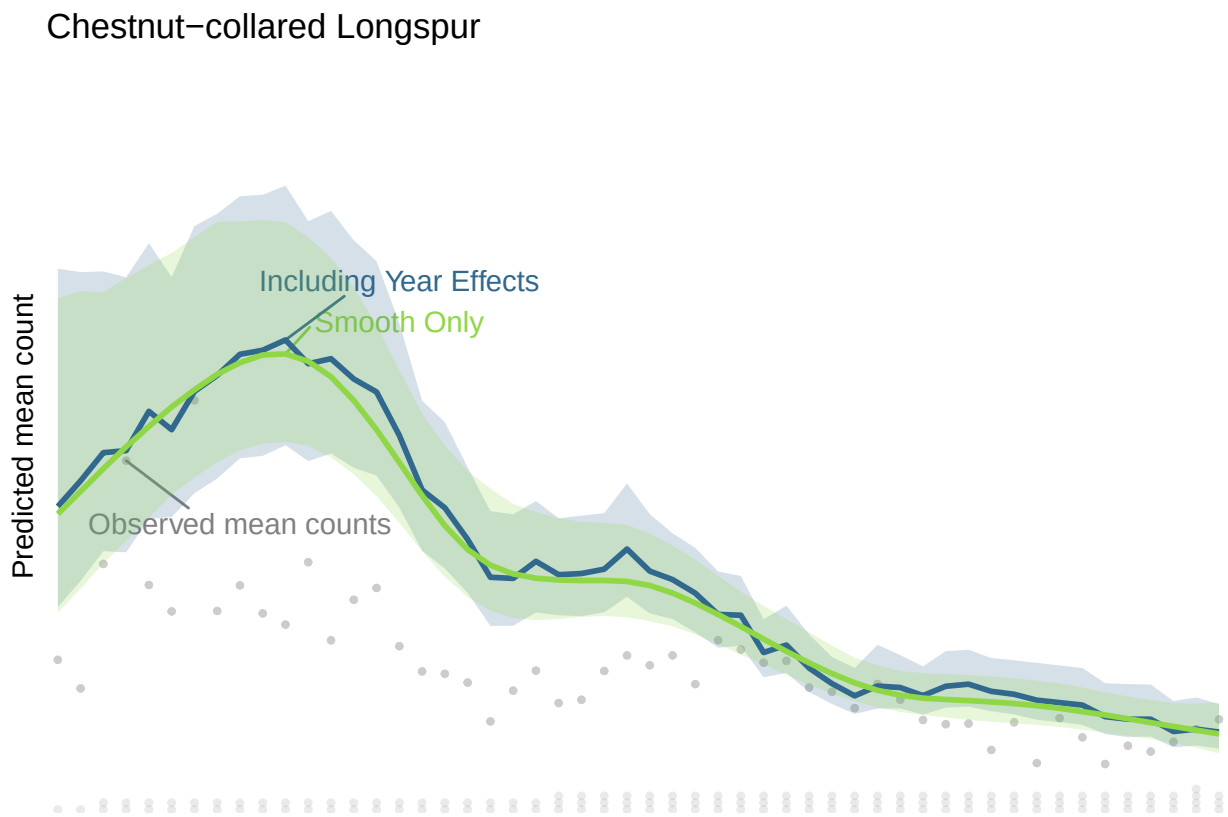

Figure 15: S5.E: Decomposition of the survey-wide population trajectory for Chestnut-collared Longspur from the GAMYE, showing the full trajectory (Including Year Effects) and the isolated smooth component (Smooth Only), which can be used to estimate population trends that are less sensitive to the particular year in which they are estimated. The stacked dots along the x axis indicate the approximate number of BBS counts used in the model; each dot represents 50 counts.

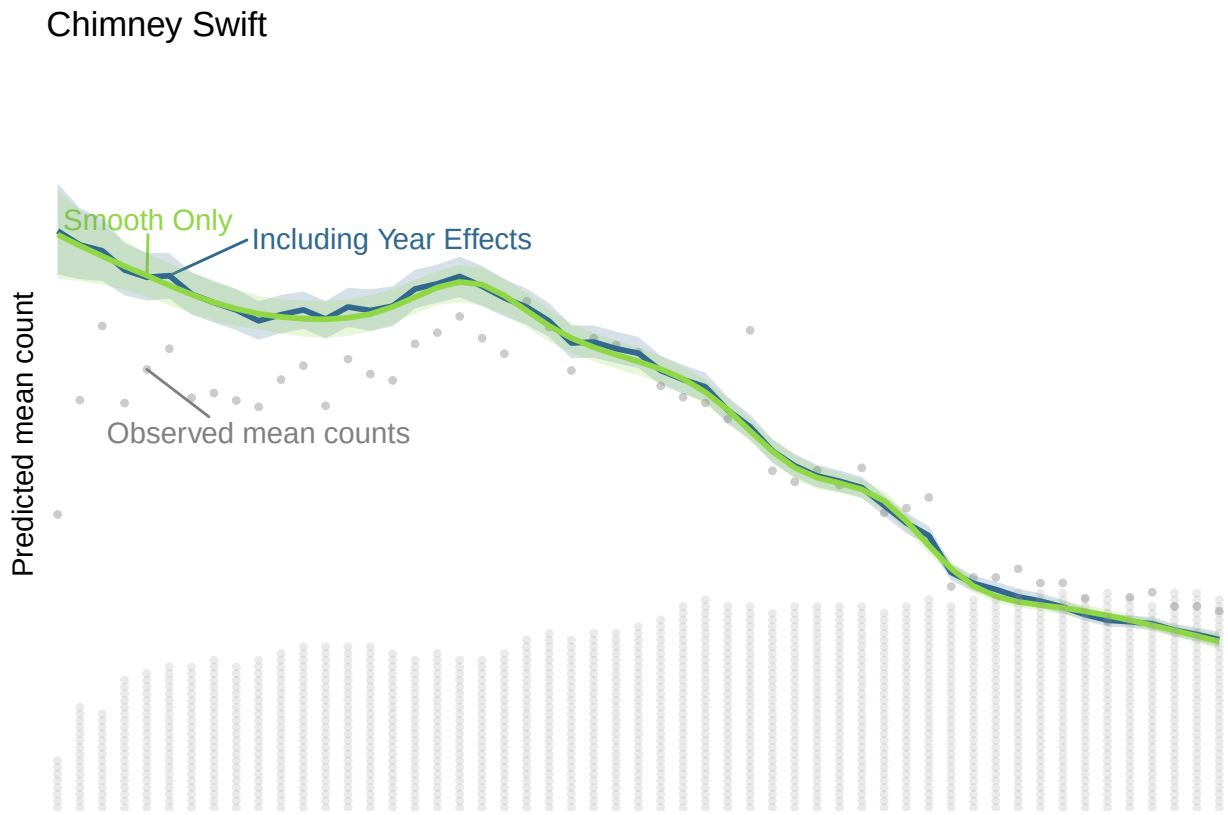

Figure 16: S5.F: Decomposition of the survey-wide population trajectory for Chimney Swift from the GAMYE, showing the full trajectory (Including Year Effects) and the isolated smooth component (Smooth Only), which can be used to estimate population trends that are less sensitive to the particular year in which they are estimated. The stacked dots along the x axis indicate the approximate number of BBS counts used in the model; each dot represents 50 counts.

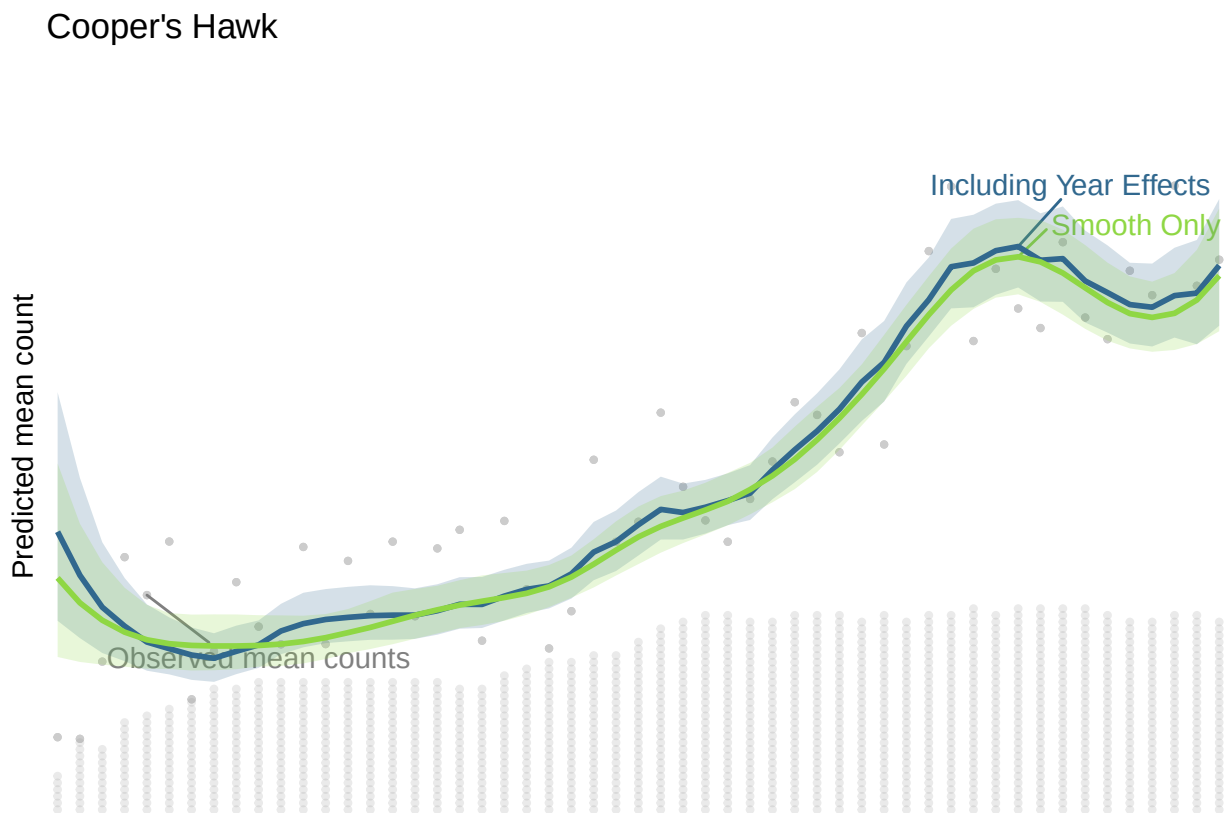

Figure 17: S5.G: Decomposition of the survey-wide population trajectory for Cooper's Hawk from the GAMYE, showing the full trajectory (Including Year Effects) and the isolated smooth component (Smooth Only), which can be used to estimate population trends that are less sensitive to the particular year in which they are estimated. The stacked dots along the x axis indicate the approximate number of BBS counts used in the model; each dot represents 50 counts.

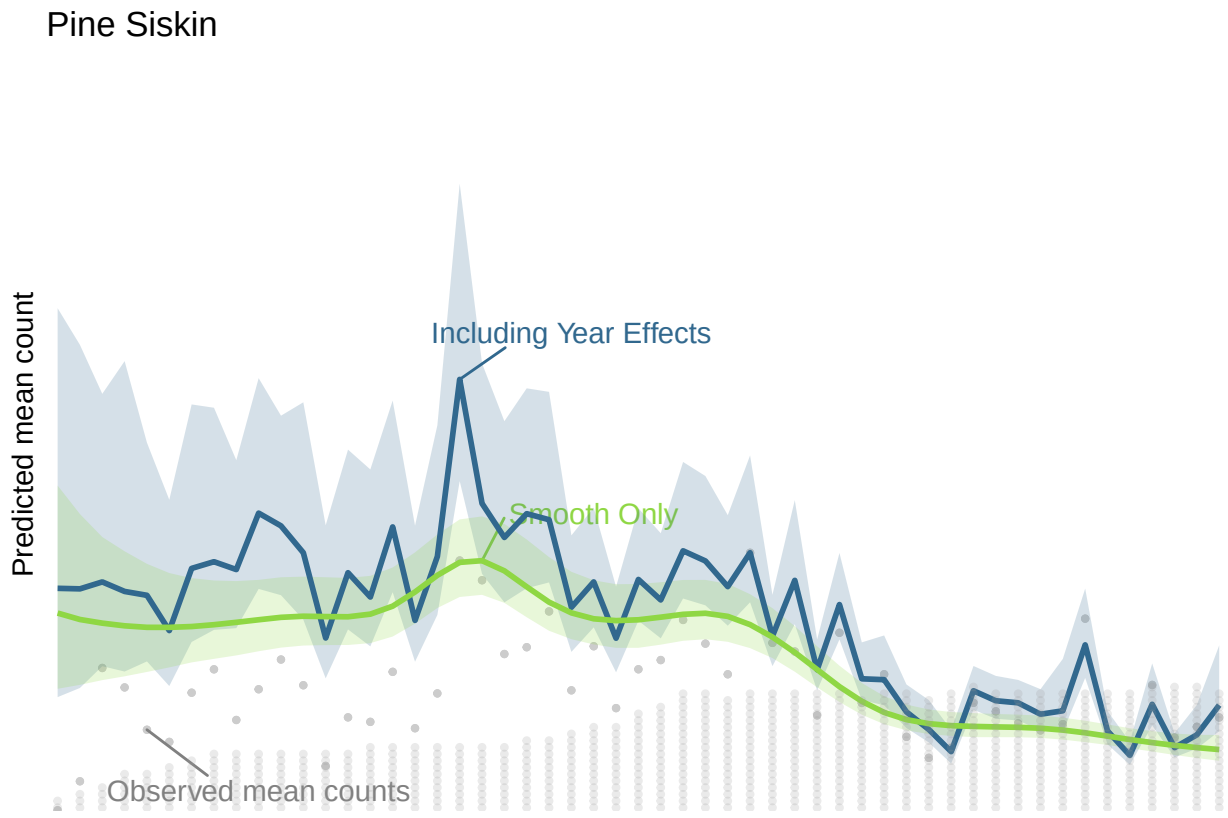

Figure 18: S5.H: Decomposition of the survey-wide population trajectory for Pine Siskin from the GAMYE, showing the full trajectory (Including Year Effects) and the isolated smooth component (Smooth Only), which can be used to estimate population trends that are less sensitive to the particular year in which they are estimated. The stacked dots along the x axis indicate the approximate number of BBS counts used in the model; each dot represents 50 counts.

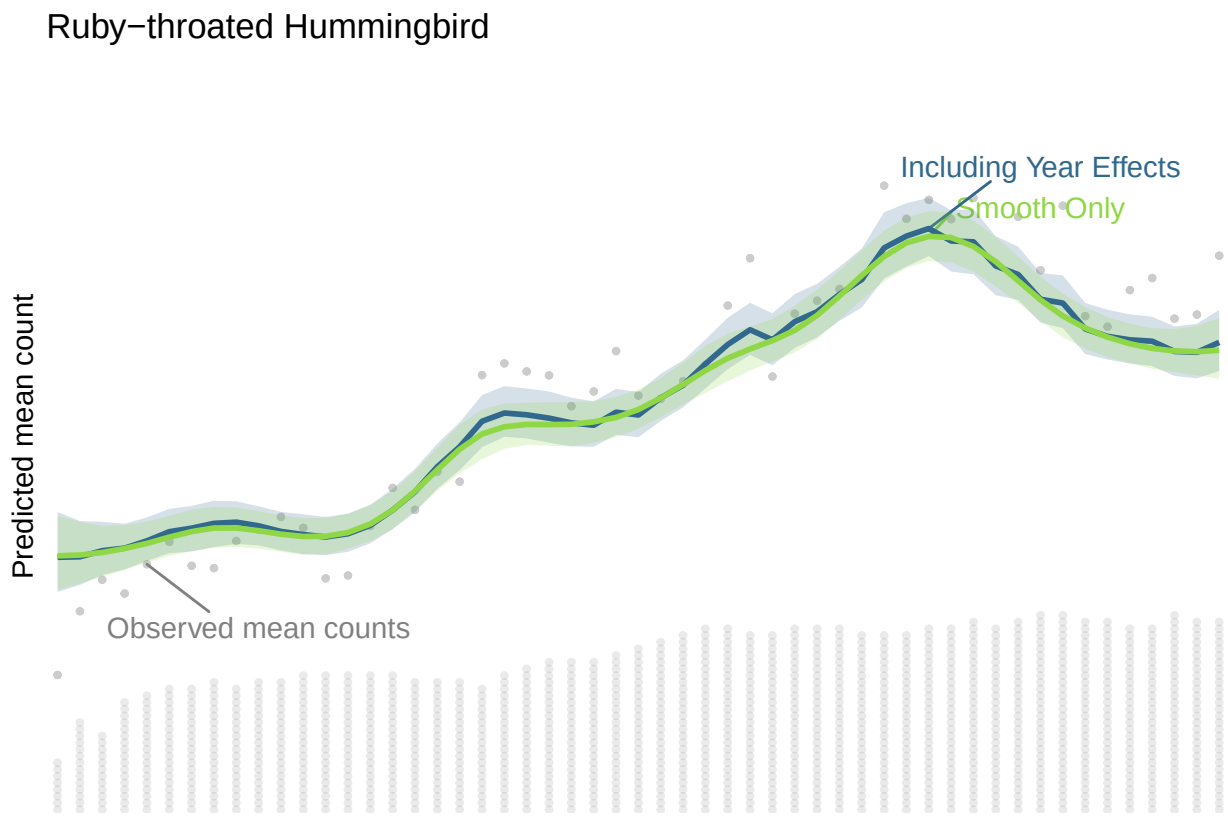

Figure 19: S5.I: Decomposition of the survey-wide population trajectory for Ruby-throated Hummingbird from the GAMYE, showing the full trajectory (Including Year Effects) and the isolated smooth component (Smooth Only), which can be used to estimate population trends that are less sensitive to the particular year in which they are estimated. The stacked dots along the x axis indicate the approximate number of BBS counts used in the model; each dot represents 50 counts.

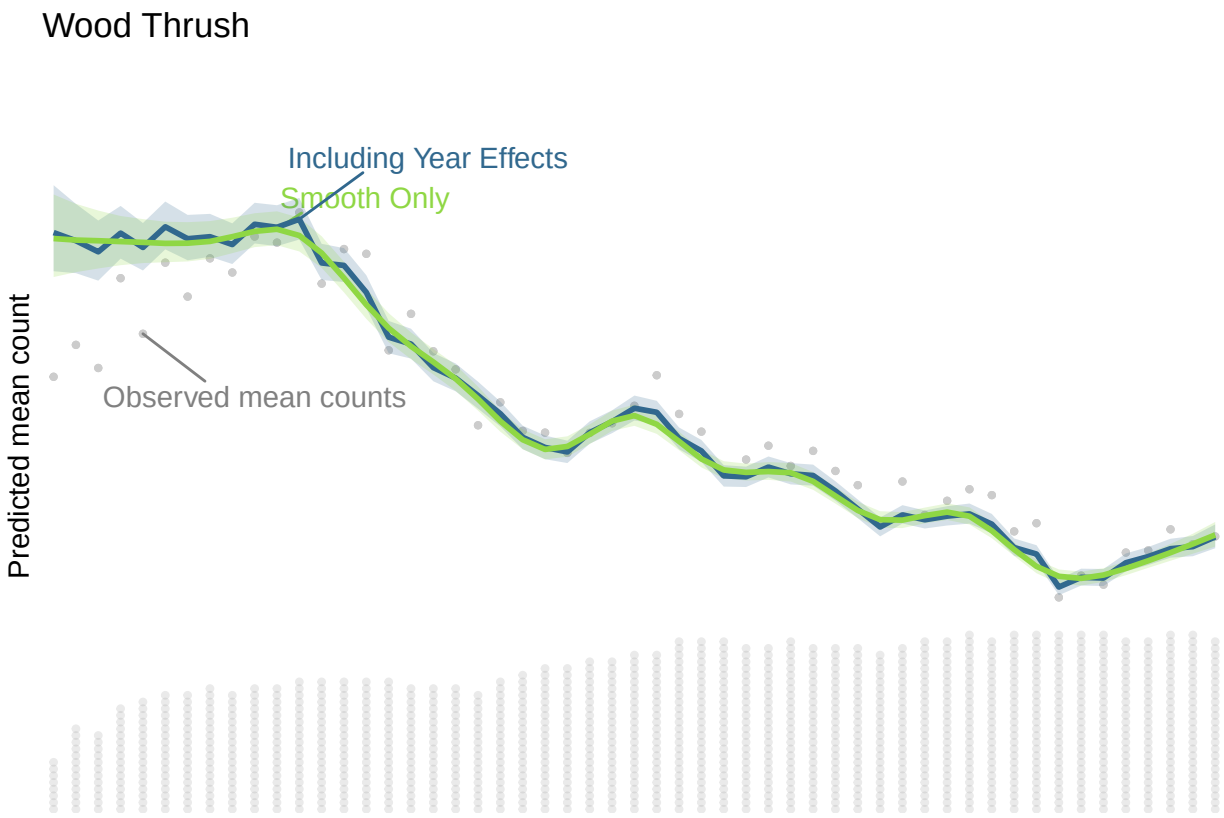
Wood Thrush
Including Year Effects
Smooth Only
Observed mean counts
Predicted mean count

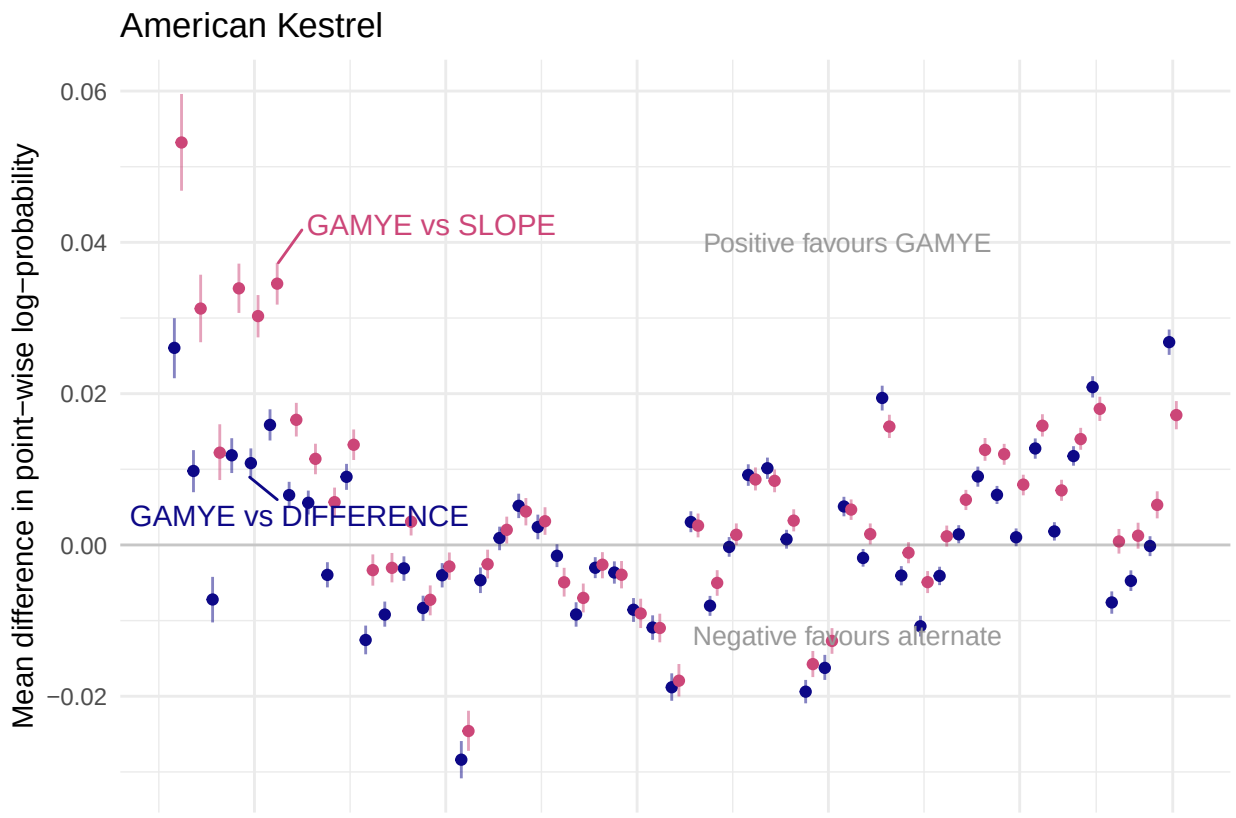

Figure 20: S6.A: Annual differences in predictive fit between the GAMYE and SLOPE (blue) and the GAMYE and DIFFERENCE model (red) for American Kestrel

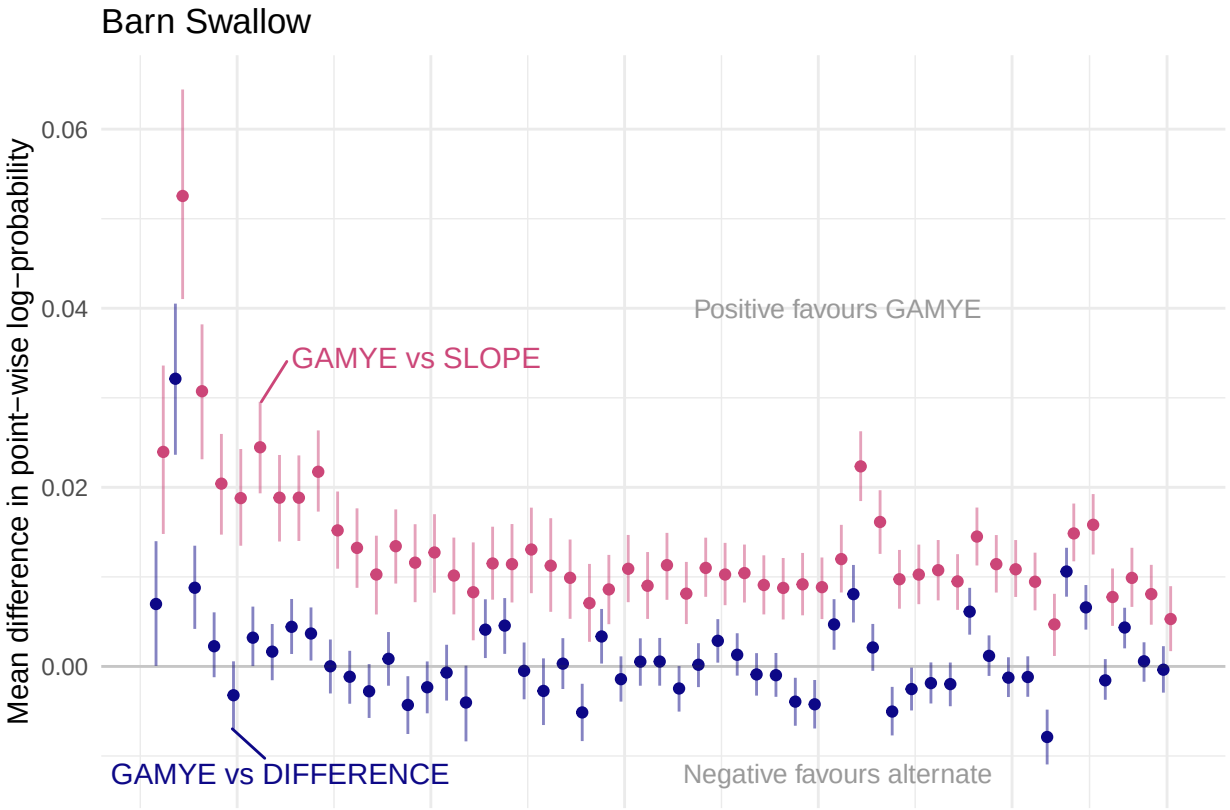

Figure 21: S6.B: Annual differences in predictive fit between the GAMYE and SLOPE (blue) and the GAMYE and DIFFERENCE model (red) for Barn Swallow

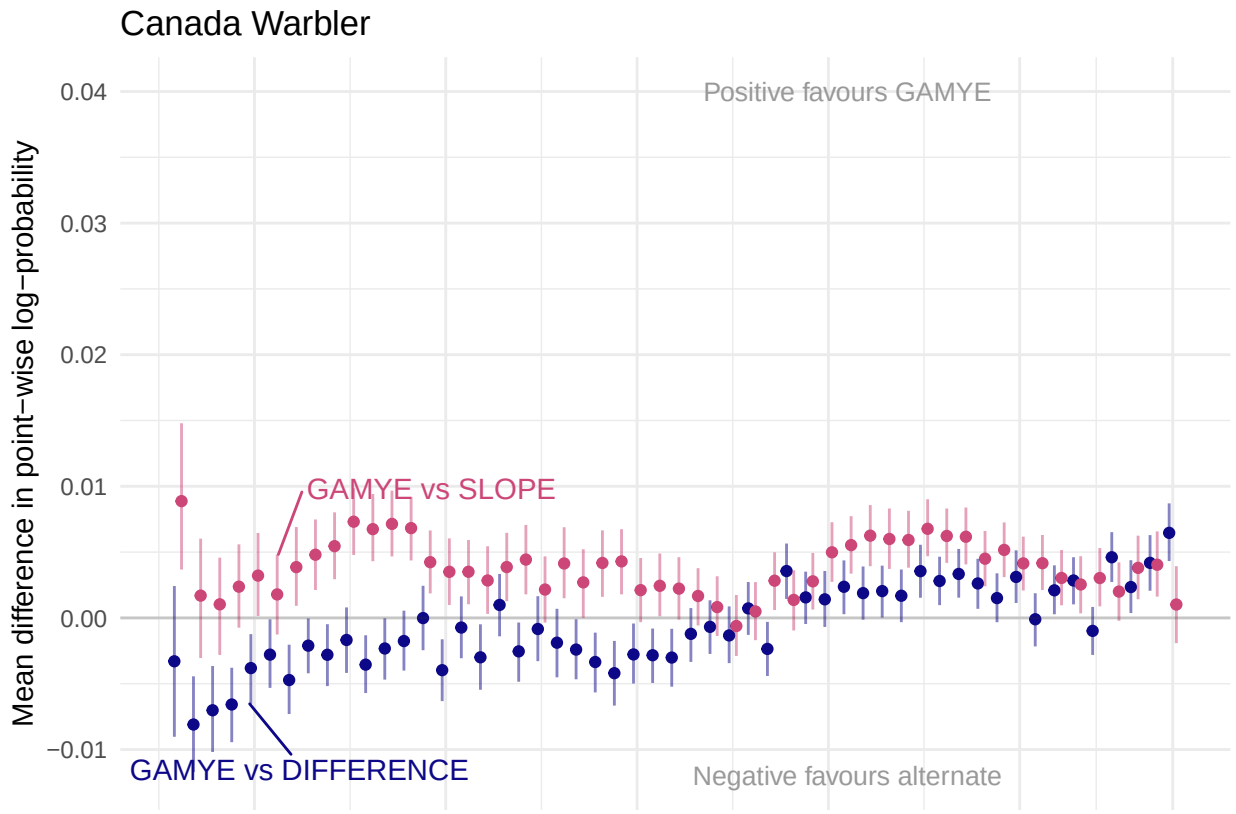

Figure 22: S6.C: Annual differences in predictive fit between the GAMYE and SLOPE (blue) and the GAMYE and DIFFERENCE model (red) for Canada Warbler

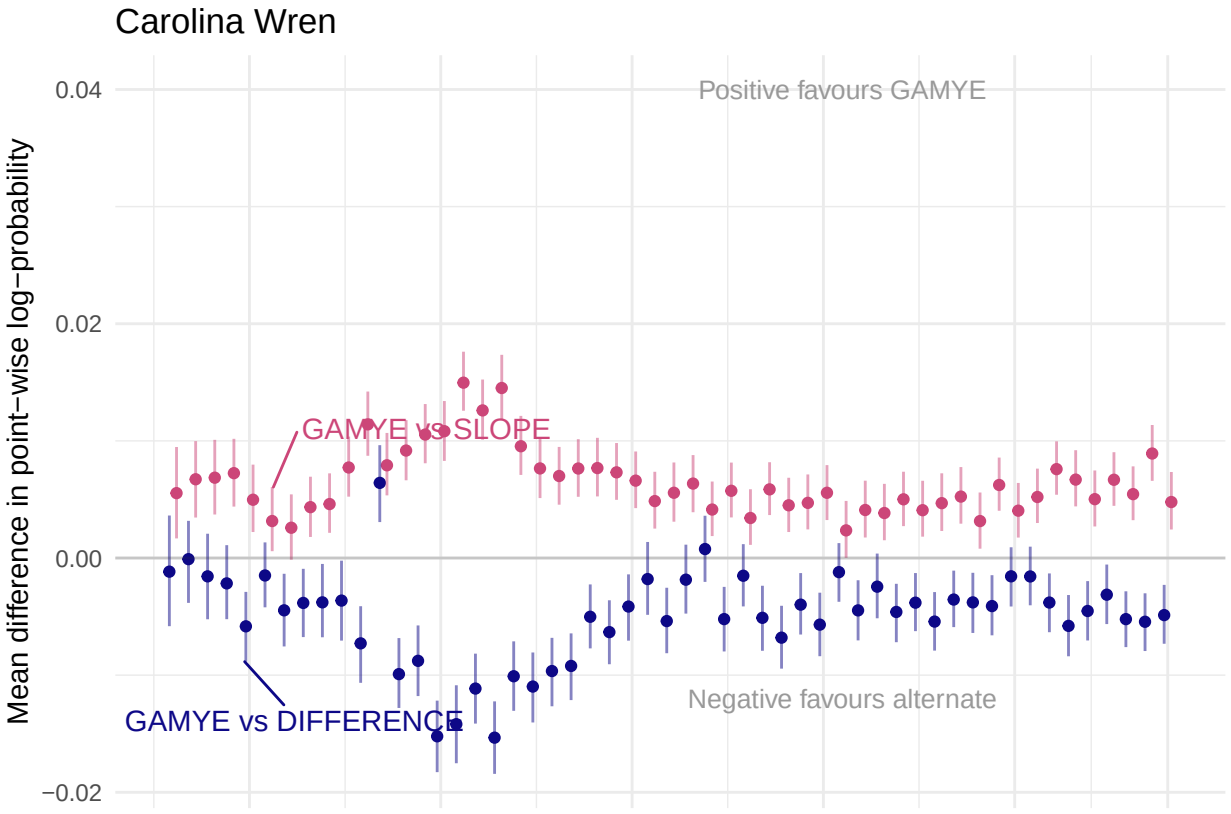

Figure 23: S6.D: Annual differences in predictive fit between the GAMYE and SLOPE (blue) and the GAMYE and DIFFERENCE model (red) for Carolina Wren

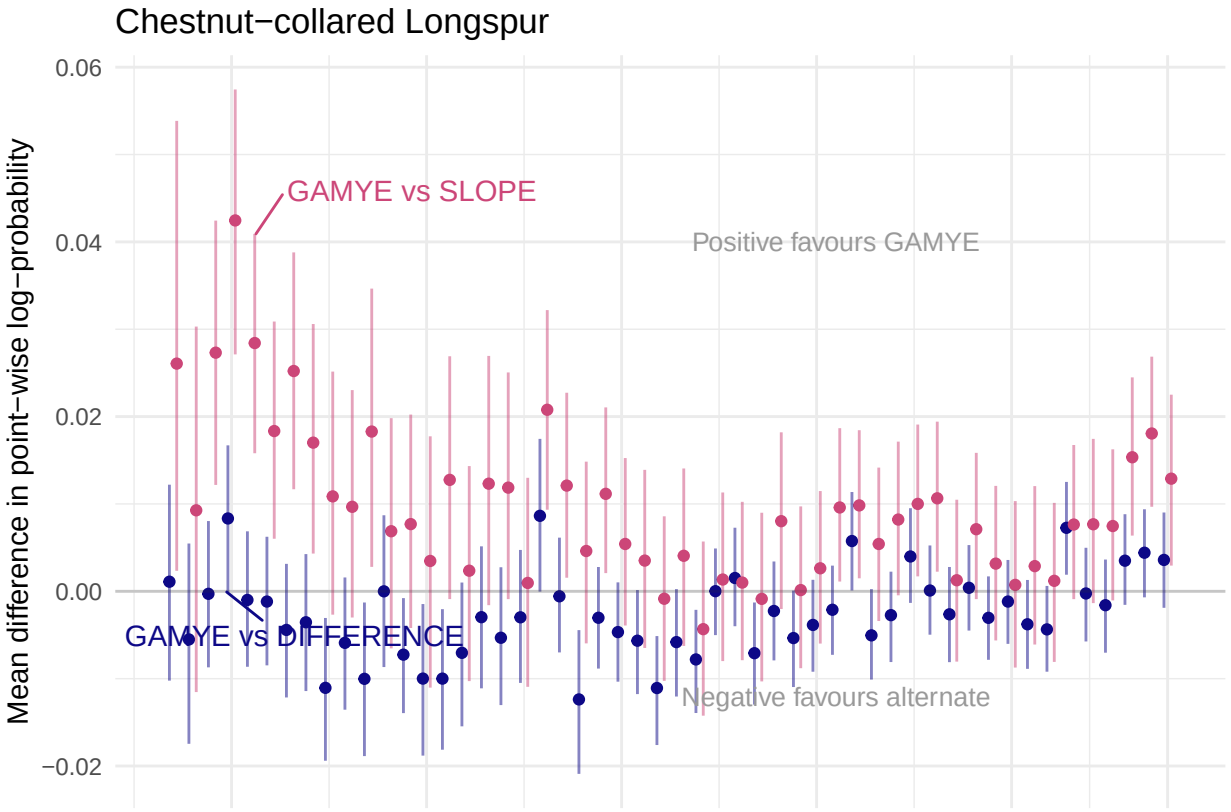

Figure 24: S6.E: Annual differences in predictive fit between the GAMYE and SLOPE (blue) and the GAMYE and DIFFERENCE model (red) for Chestnut-collared Longspur

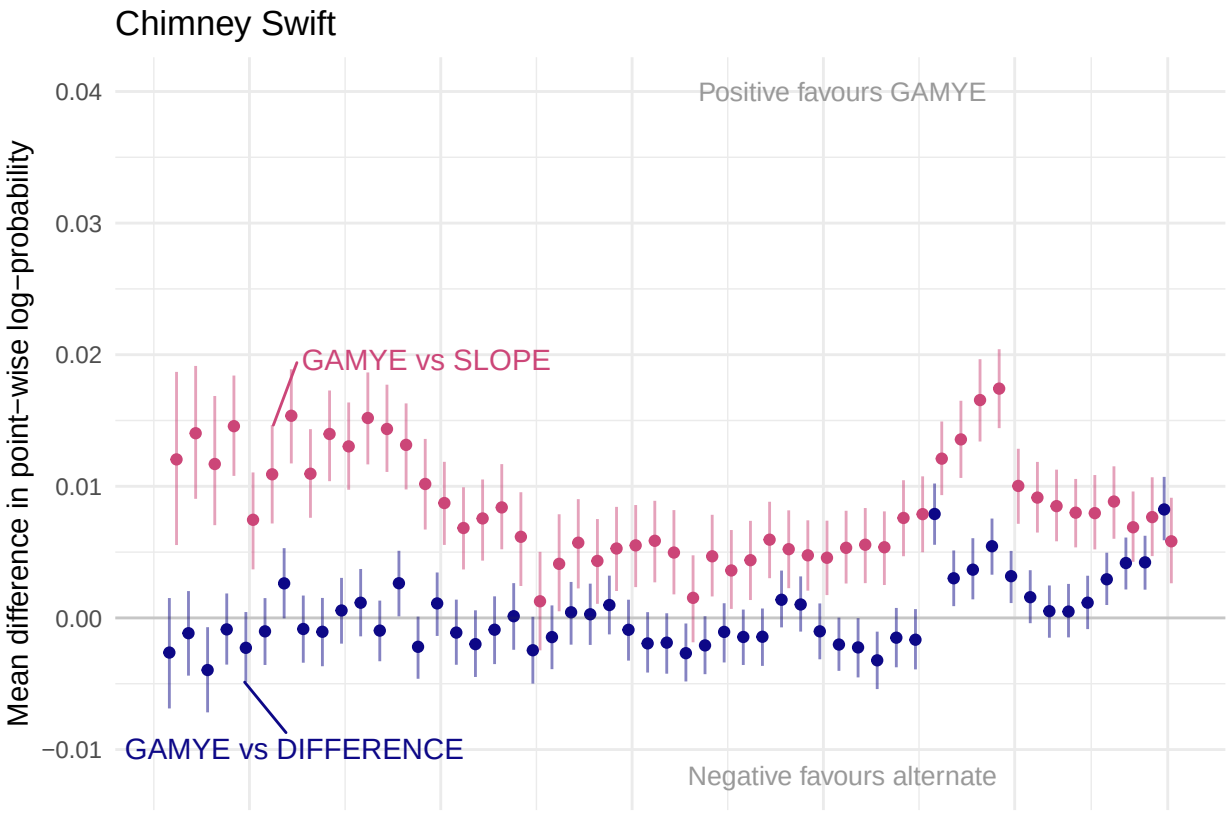

Figure 25: S6.F: Annual differences in predictive fit between the GAMYE and SLOPE (blue) and the GAMYE and DIFFERENCE model (red) for Chimney Swift

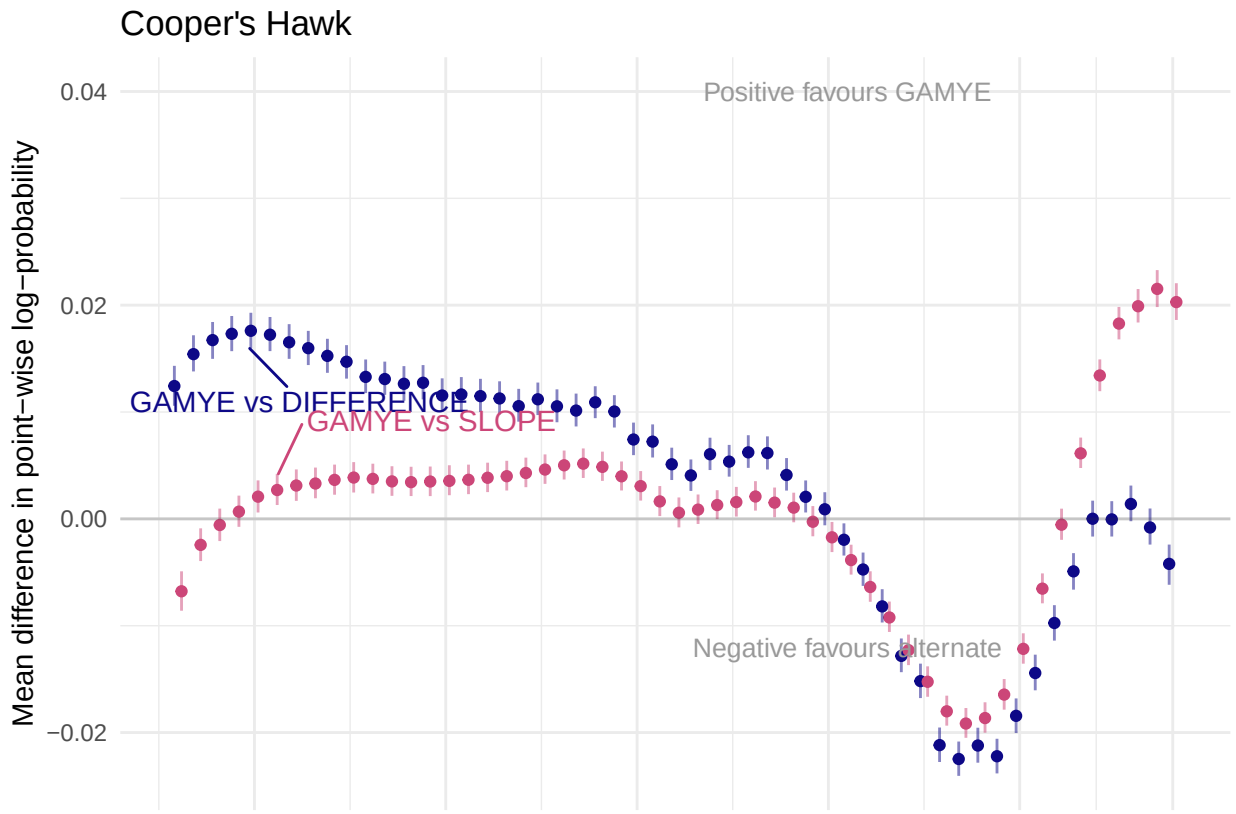

Figure 26: S6.G: Annual differences in predictive fit between the GAMYE and SLOPE (blue) and the GAMYE and DIFFERENCE model (red) for Cooper's Hawk

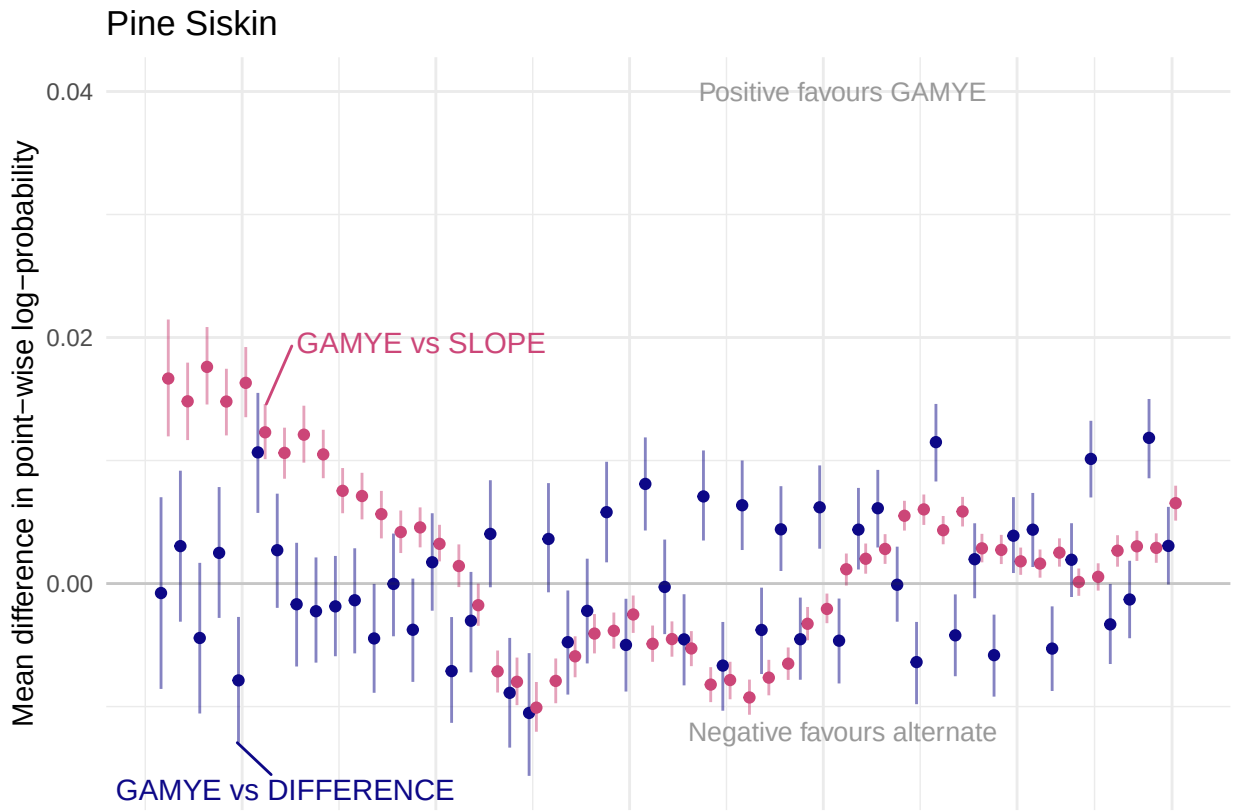

Figure 27: S6.H: Annual differences in predictive fit between the GAMYE and SLOPE (blue) and the GAMYE and DIFFERENCE model (red) for Pine Siskin

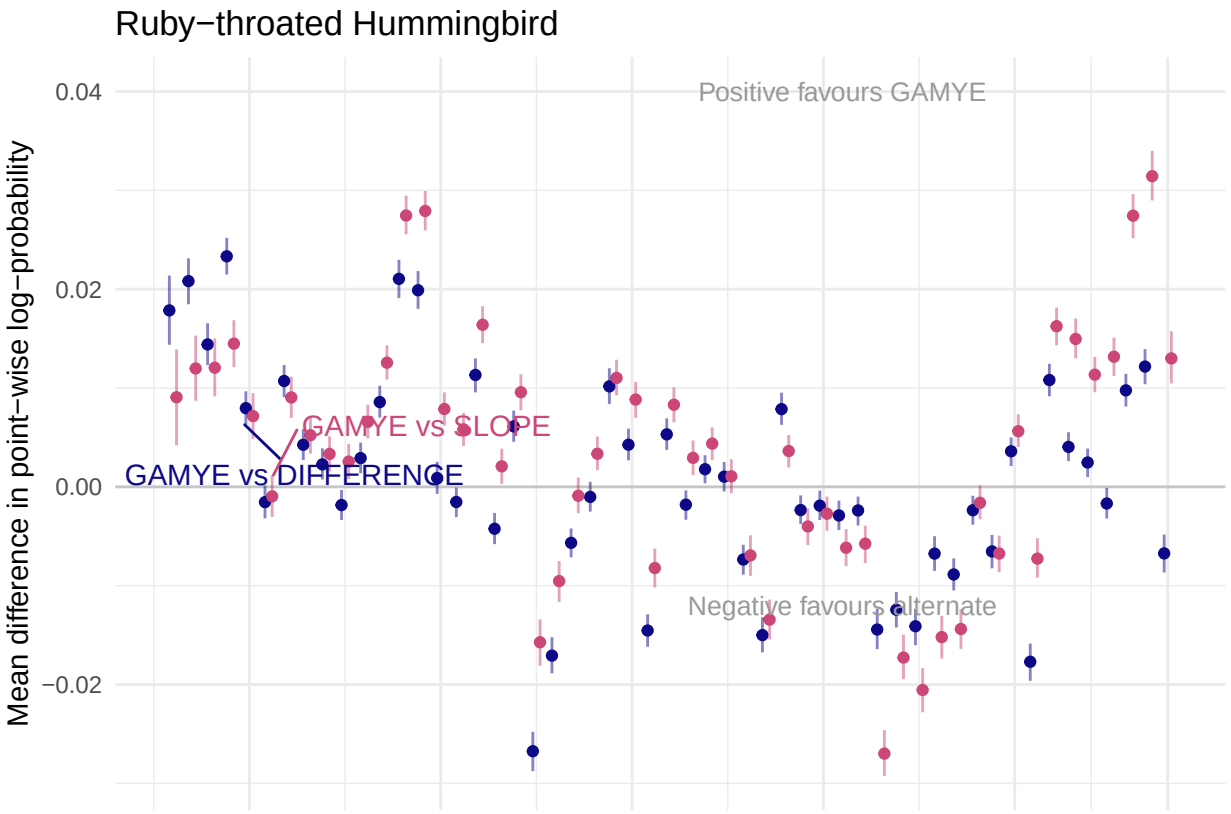

Figure 28: S6.I: Annual differences in predictive fit between the GAMYE and SLOPE (blue) and the GAMYE and DIFFERENCE model (red) for Ruby-throated Hummingbird

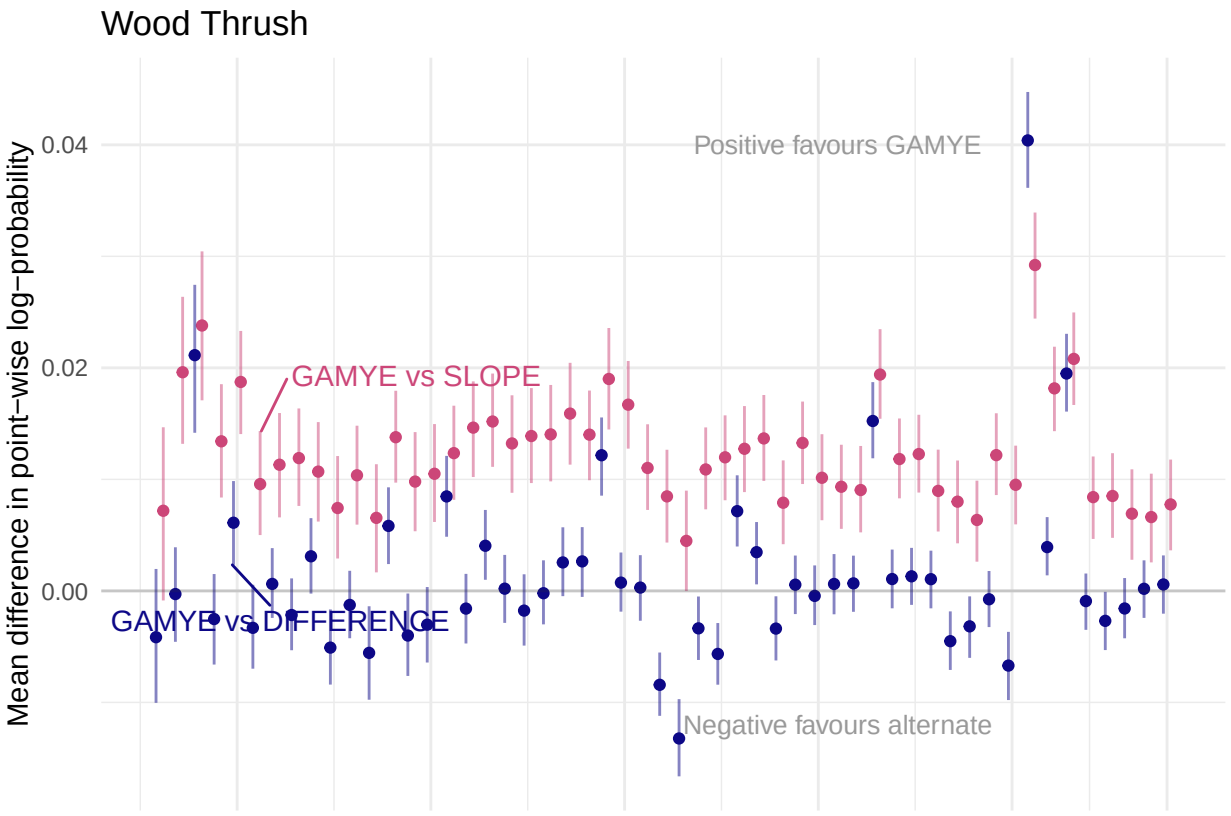
Wood Thrush
Mean difference in point−wise log−probability
0.04
0.02
0.00
Positive favours GAMYE
GAMYE vs SLOPE
GAMYE vs DIFFERENCE
Negative favours alternate

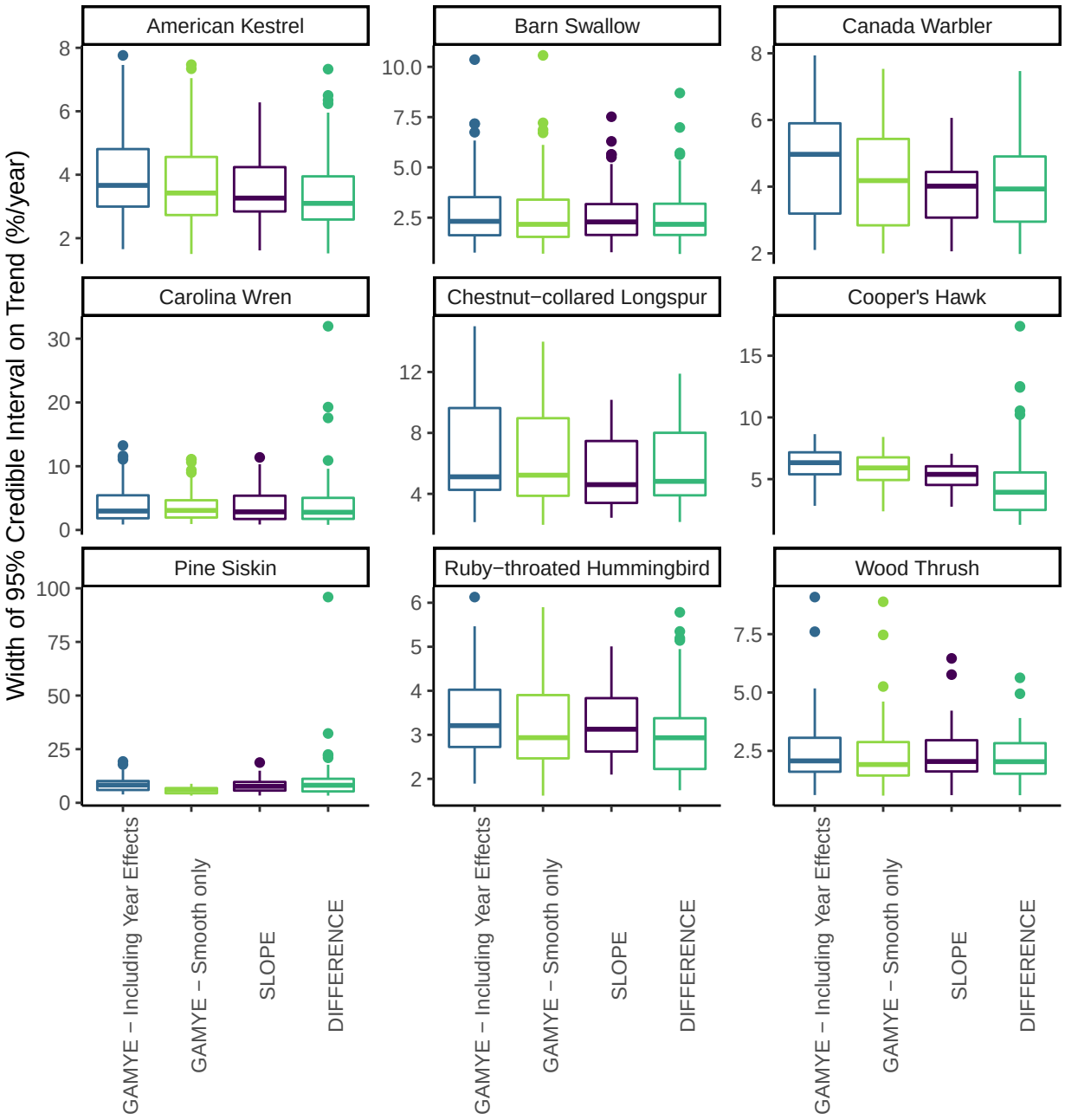
American Kestrel
Barn Swallow
Canada Warbler
Carolina Wren
Chestnut−collared Longspur
Cooper's Hawk
Pine Siskin
Ruby−throated Hummingbird
Wood Thrush
Width of 95% Credible Interval on Trend (%/year)
GAMYE – Including Year Effects
GAMYE – Smooth only
SLOPE
DIFFERENCE

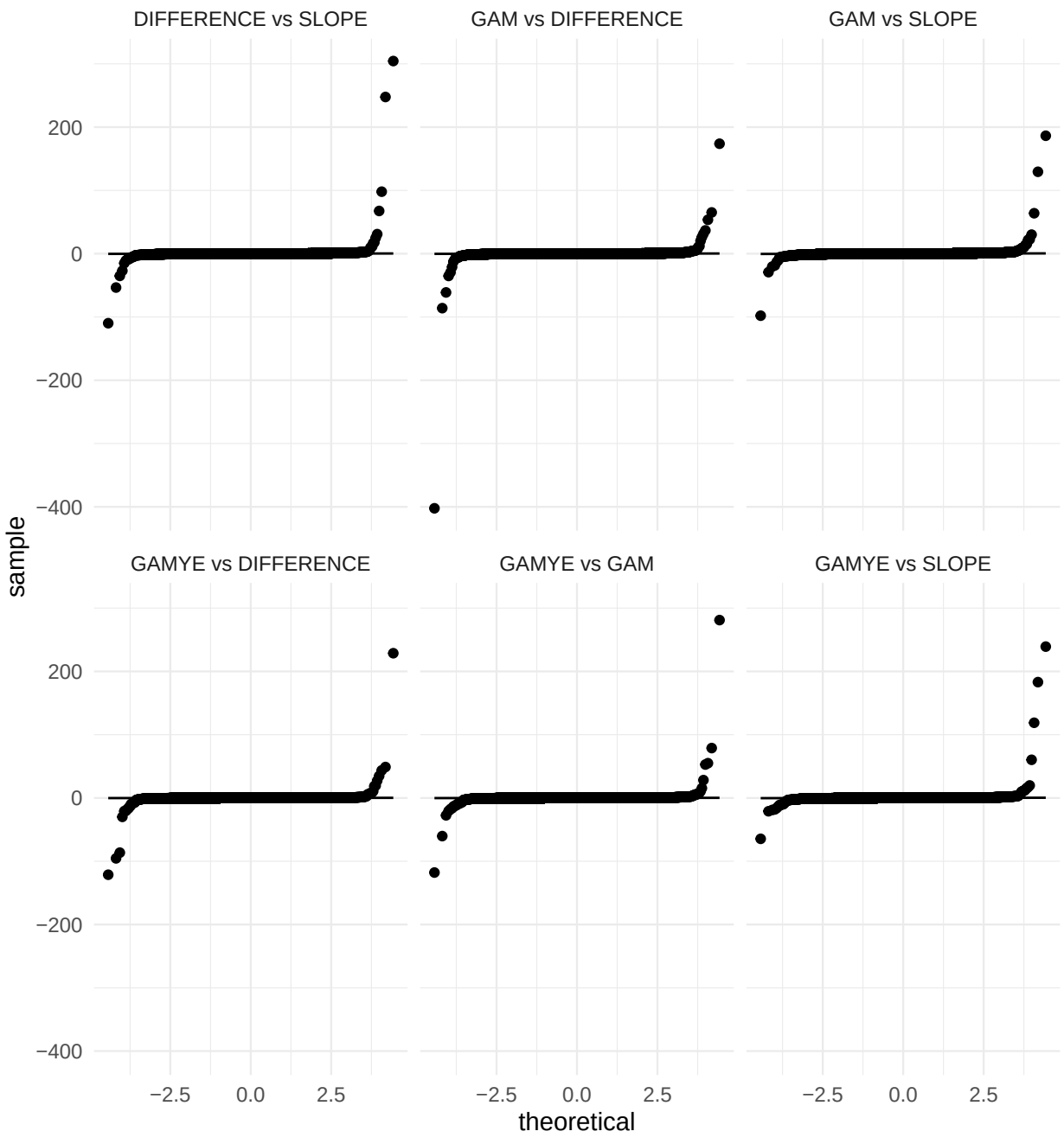

Figure 29: Figure S7: Normal qq plots for the differences in elpd between model pairs for Barn Swallow, demonstrating the non-normal distribution and the heavy tails better estimated using a t-distribution

Assessing the prior sensitivity of the GAM hyperparameters

The inverse gamma prior on the variance of the GAM hyperparameters follows the recommended priors in Crainiceanu et al. 2005 (~gamma(0.01,0.0001)). If transformed to the scale of the standard deviation, the 99% percentile of the prior distribution is > 10^100. This prior is intended to be uninformative because it is effectively flat across the entire range of plausible values (< approximately 5). However, this prior also includes values of the variance (or standard deviation) that are far beyond the range of plausible values. The posterior distribution of this variance parameter is largely responsible for the complexity penalty, controlling the degree of smoothing in the GAM, and so if the prior is unintentionally informative, it could result in under-restrictive smoothing penalties. If this "uninformative" prior is leading to under-restrictive smoothing, it would produce population trajectories that over-fit the data and appear more complex (i.e., "wiggly") than warranted. The figures below show that using a much more restrictive prior (~gamma(2,0.2)) that places > 99% of the posterior density for the standard deviation at values < 1.2. For most species, this is a regularizing prior because almost all of the prior density falls below the posterior estimates, which are generally > 2.0. So the two priors are very different, yet as the following figures demonstrate, the posterior estimates of the GAM trajectories are almost identical. The population inferences from the GAMs are almost entirely driven by the model-structures and the data.

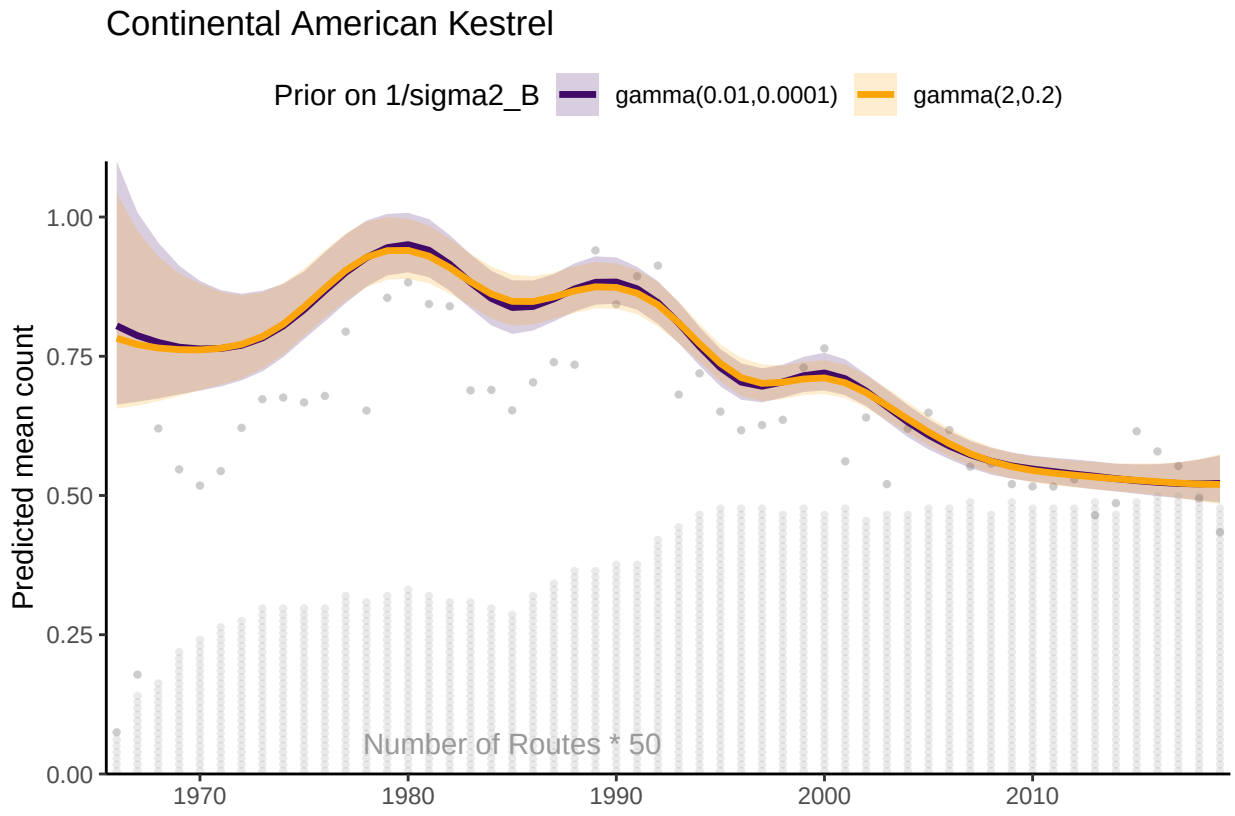

Figure 30: S7.A: Comparison of the continental population trajectories for American Kestrel from a model for the BBS using a hierarchical GAM smooth with two alternative prior distributions on the variance parameter that provides the complexity penalty for the survey-wide GAM hyperparameters, i.e., the mean continental population trajectory towards which each stratum-level smooth is shrunk

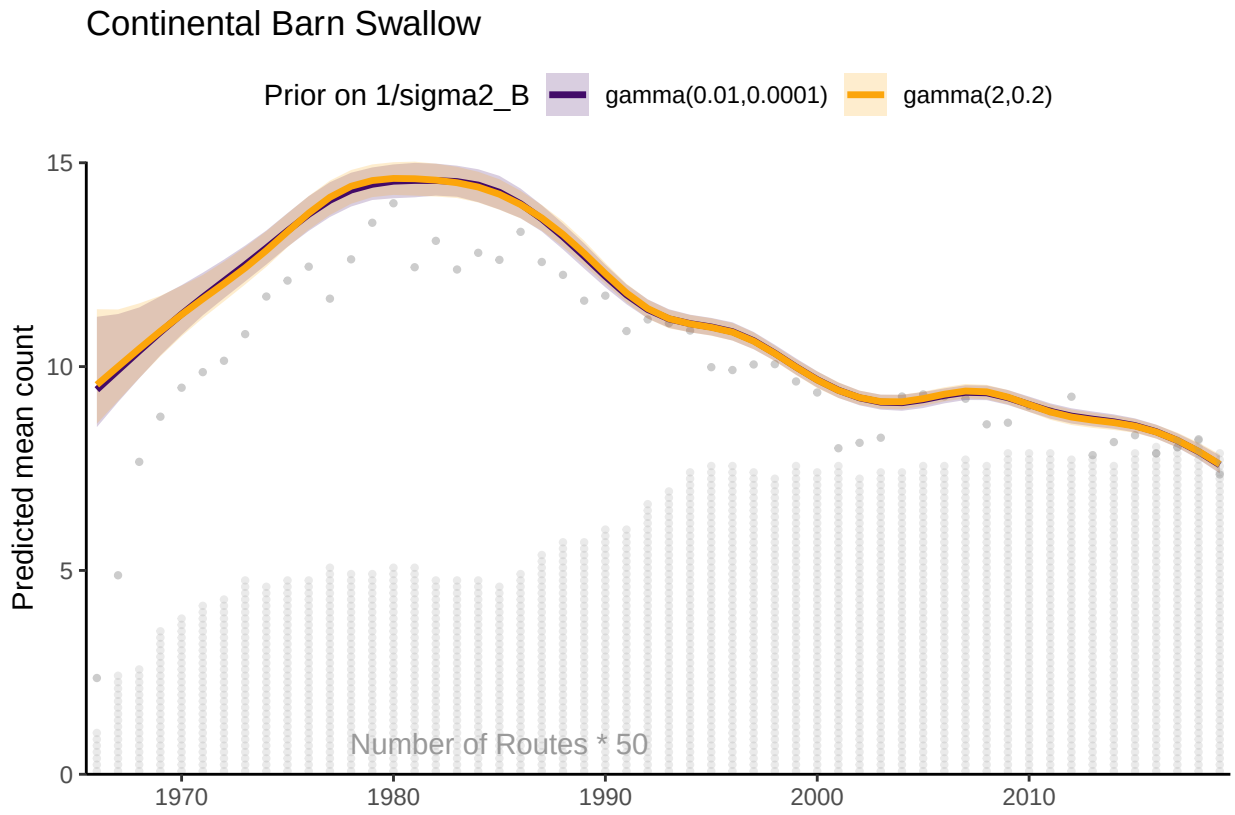

Figure 31: S8.A: Comparison of the continental population trajectories for Barn Swallow from a model for the BBS using a hierarchical GAM smooth with two alternative prior distributions on the variance parameter that provides the complexity penalty for the survey-wide GAM hyperparameters, i.e., the mean continental population trajectory towards which each stratum-level smooth is shrunk

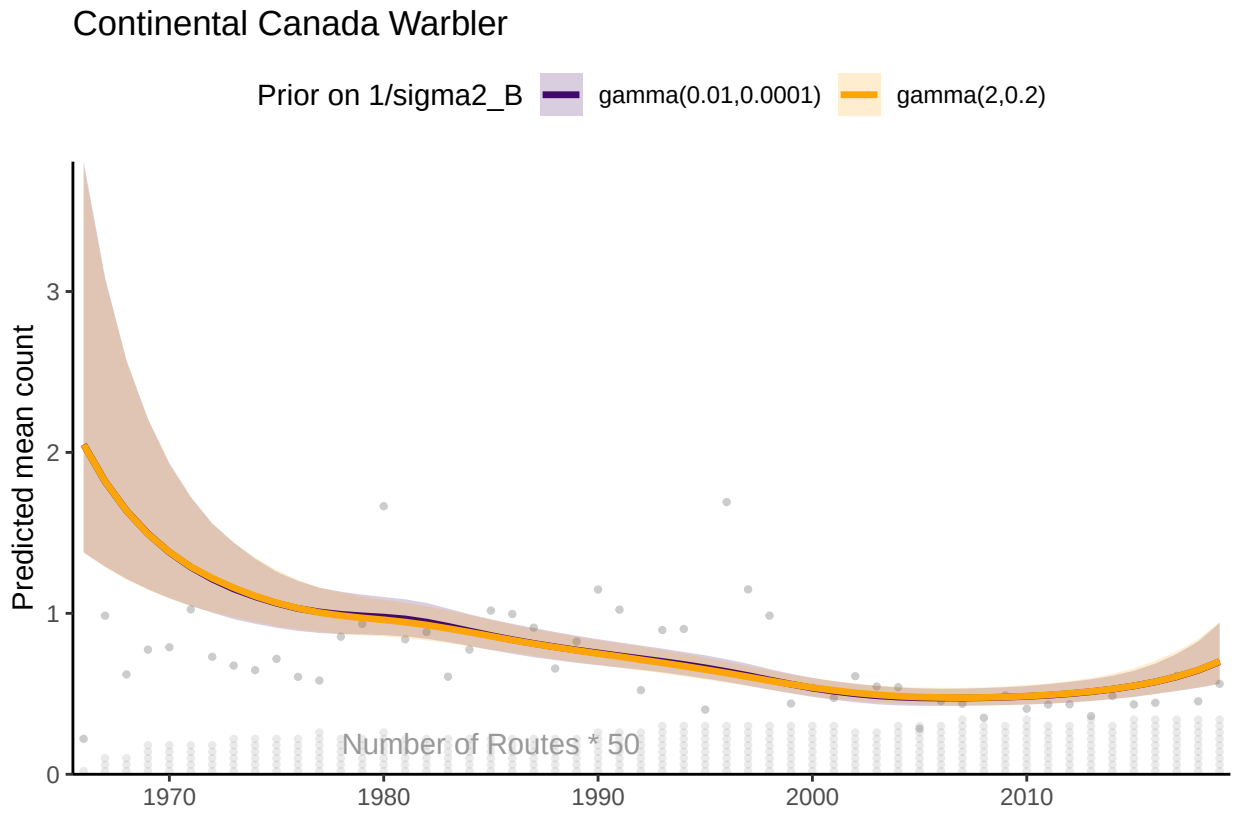

Figure 32: S9.A: Comparison of the continental population trajectories for Canada Warbler from a model for the BBS using a hierarchical GAM smooth with two alternative prior distributions on the variance parameter that provides the complexity penalty for the survey-wide GAM hyperparameters, i.e., the mean continental population trajectory towards which each stratum-level smooth is shrunk

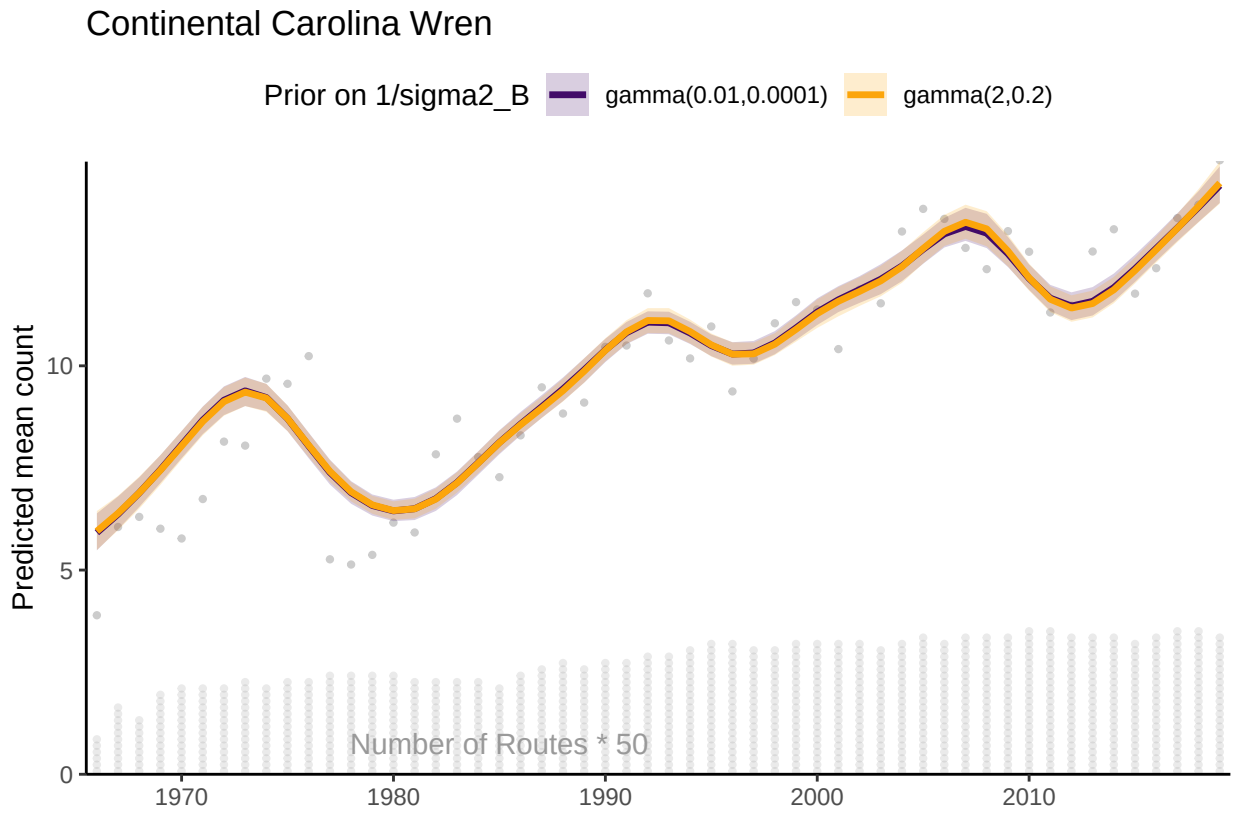

Figure 33: S9.B: Comparison of the continental population trajectories for Carolina Wren from a model for the BBS using a hierarchical GAM smooth with two alternative prior distributions on the variance parameter that provides the complexity penalty for the survey-wide GAM hyperparameters, i.e., the mean continental population trajectory towards which each stratum-level smooth is shrunk

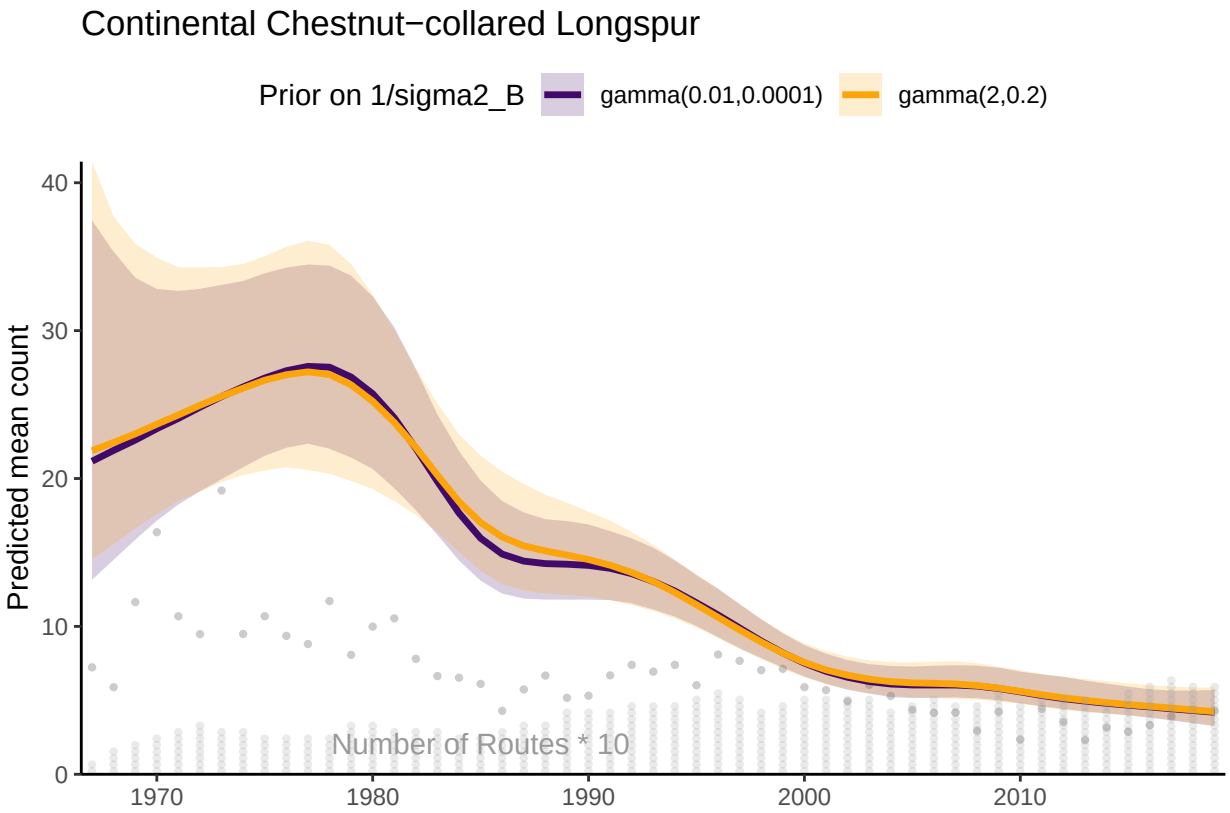

Figure 34: S9.C: Comparison of the continental population trajectories for Chestnut-collared Longspur from a model for the BBS using a hierarchical GAM smooth with two alternative prior distributions on the variance parameter that provides the complexity penalty for the survey-wide GAM hyperparameters, i.e., the mean continental population trajectory towards which each stratum-level smooth is shrunk

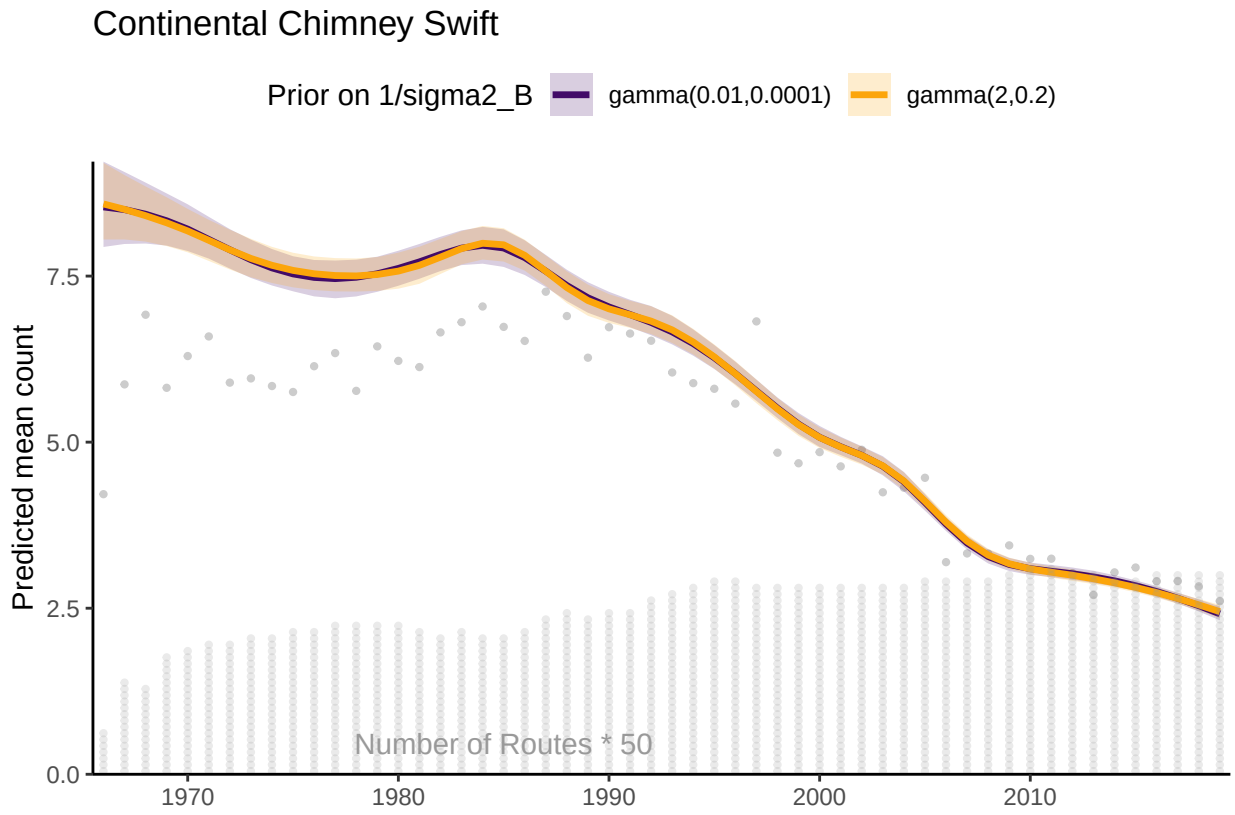

Figure 35: S9.D: Comparison of the continental population trajectories for Chimney Swift from a model for the BBS using a hierarchical GAM smooth with two alternative prior distributions on the variance parameter that provides the complexity penalty for the survey-wide GAM hyperparameters, i.e., the mean continental population trajectory towards which each stratum-level smooth is shrunk

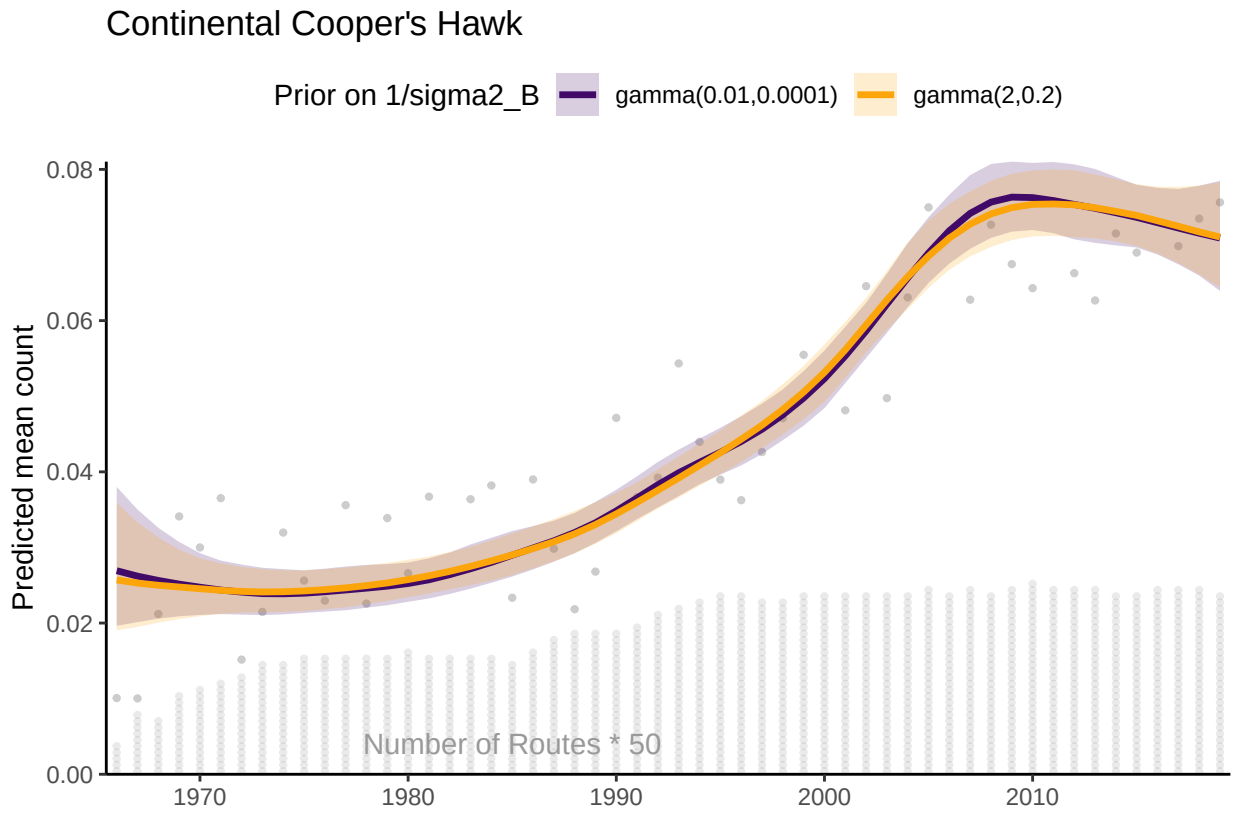

Figure 36: S9.E: Comparison of the continental population trajectories for Cooper's Hawk from a model for the BBS using a hierarchical GAM smooth with two alternative prior distributions on the variance parameter that provides the complexity penalty for the survey-wide GAM hyperparameters, i.e., the mean continental population trajectory towards which each stratum-level smooth is shrunk

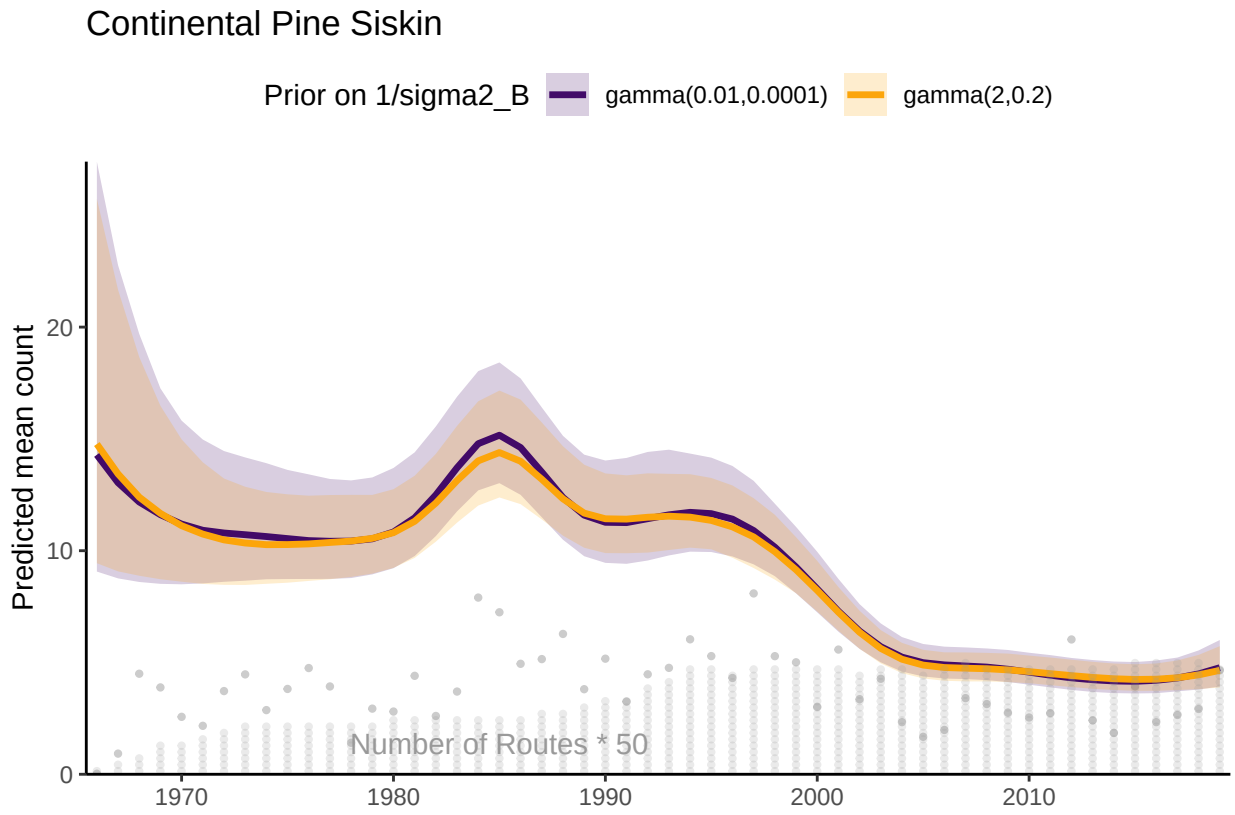

Figure 37: S9.F: Comparison of the continental population trajectories for Pine Siskin from a model for the BBS using a hierarchical GAM smooth with two alternative prior distributions on the variance parameter that provides the complexity penalty for the survey-wide GAM hyperparameters, i.e., the mean continental population trajectory towards which each stratum-level smooth is shrunk

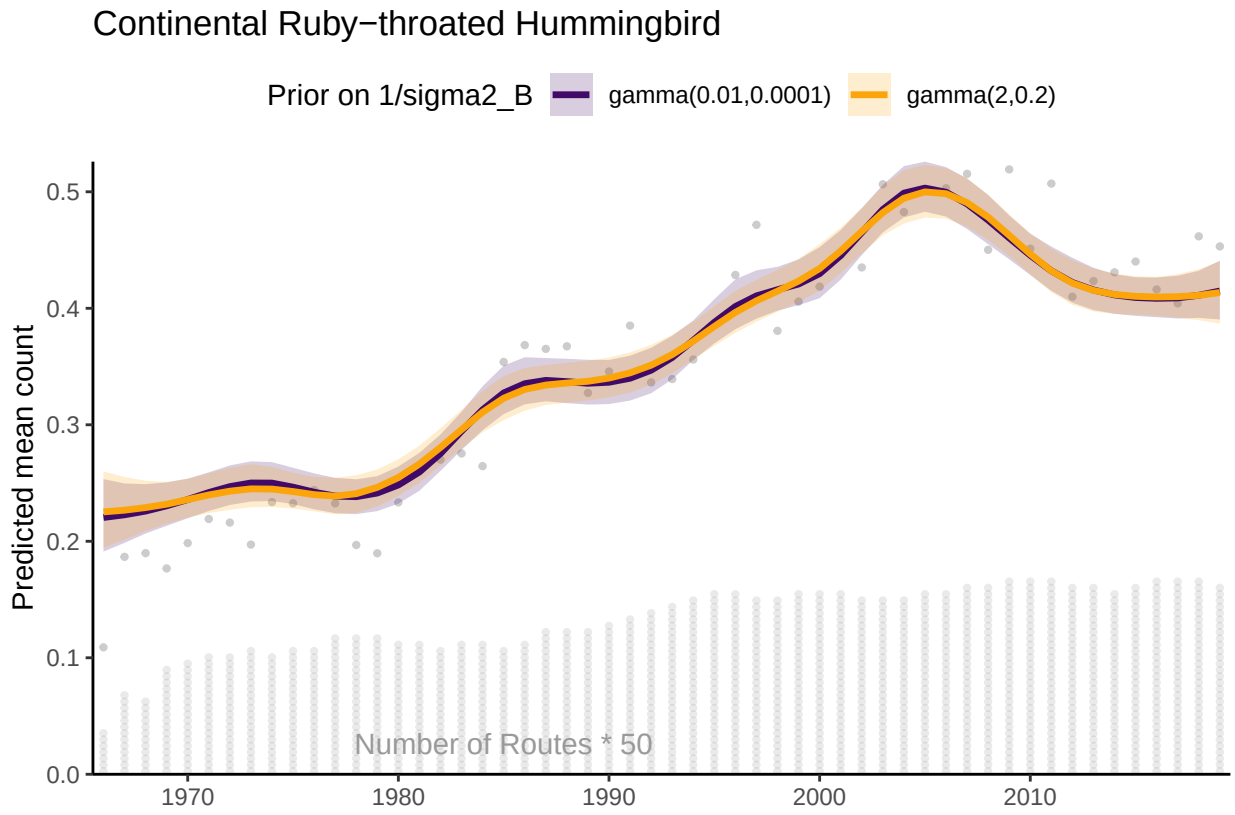

Figure 38: S9.G: Comparison of the continental population trajectories for Ruby-throated Hummingbird from a model for the BBS using a hierarchical GAM smooth with two alternative prior distributions on the variance parameter that provides the complexity penalty for the survey-wide GAM hyperparameters, i.e., the mean continental population trajectory towards which each stratum-level smooth is shrunk

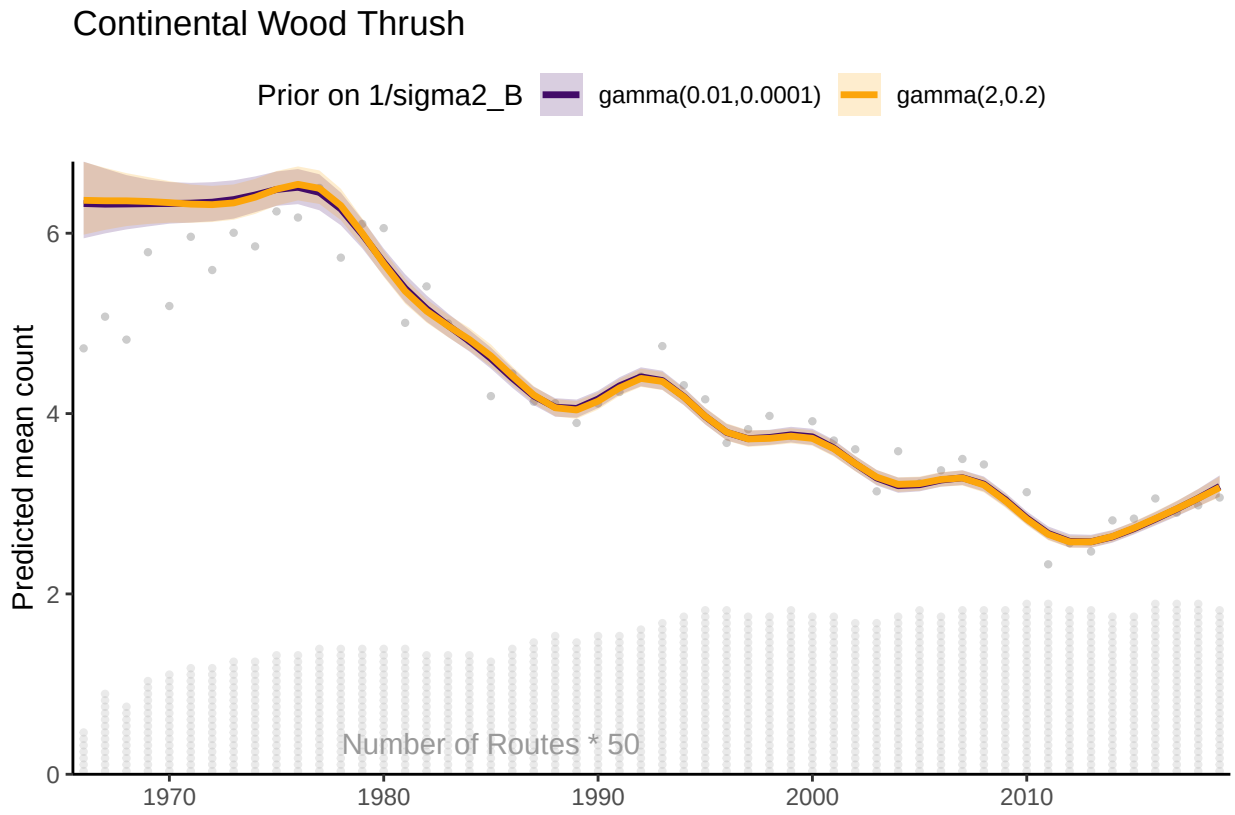

Figure 39: S9.H: Comparison of the continental population trajectories for Wood Thrush from a model for the BBS using a hierarchical GAM smooth with two alternative prior distributions on the variance parameter that provides the complexity penalty for the survey-wide GAM hyperparameters, i.e., the mean continental population trajectory towards which each stratum-level smooth is shrunk